

Abstract

The Iberia-Biscay-Ireland (IBI) system serves one of the 7 MyOcean “Monitoring and Forecasting Centres”. A high resolution simulation covering the IBI region is set-up over July 2007–February 2009. The NEMO (Nucleus for European Modelling of the Ocean) model is used with a $1/36^\circ$ horizontal resolution and 50 z-levels in the vertical. New developments have been incorporated in NEMO to make it suitable to open- as well as coastal-ocean modelling. In this paper, we pursue three main objectives: (1) give an overview of the model configuration used for the simulations; (2) give a broad-brush account of one particular aspect of this work, namely consistency verification; this type of validation is conducted upstream of the implementation of the system before it is used for production and routinely validated; it is meant to guide model development in identifying gross deficiencies in the modelling of several key physical processes; (3) show that such a regional modelling system has potential as a complement to patchy observations (an integrated approach) to give information on non-observed physical quantities and to provide links between observations by identifying broader-scale patterns and processes. We concentrate on the year 2008. We first provide domain-wide consistency verification results in terms of barotropic tides, transports, sea surface temperature and stratification. We then focus on two dynamical sub-regions: the Celtic shelves and the Bay of Biscay slope and deep regions. The model-data consistency is checked for variables and processes such as tidal currents, tidal fronts, internal tides, residual elevation. We also examine the representation in the model of a seasonal pattern of the Bay of Biscay circulation: the warm extension of the Iberian Poleward Current along the northern Spanish coast (Navidad event) in winter 2007–2008.

Assessment of the Iberia-Biscay-Ireland configuration

C. Maraldi et al.

Title Page

Abstract

Introduction

Conclusions

References

Tables

Figures



Back

Close

Full Screen / Esc

Printer-friendly Version

Interactive Discussion



1 Introduction

The North East Atlantic (NEATL) region covers areas of important economic and social activities that include fisheries, transportation of oil and gas, commercial ship traffic, coastal management, coastal protection and energy production. The increasing number of users over this region demands that good estimates and forecasts of marine variables are available in order to support the development of these activities. The Iberia-Biscay-Ireland (IBI) regional modelling system is one of the 7 MyOcean Monitoring and Forecasting Centres (<http://www.myocean.eu>), and has been developed with those needs in mind. The MyOcean and MyOcean2 projects aim at developing Marine Core Services within the GMES initiative (Global Monitoring for Environment and Security). The IBI system is to serve downstream coastal modelling users and hence contribute to the development of better products for final users. The operational version of the IBI system described in this paper is now run daily, feeding the MyOcean data access portal with daily analyses and forecasts.

The IBI modelling domain (Fig. 1) has the singular property to concentrate a large spectrum of physical ocean processes, including for instance large eddies spawned by the North Atlantic Current and the Azores Current, intense upwellings along Portuguese coasts, gravity currents flowing down Gibraltar and Faroe Channels. Characteristic to the region is a relatively steep slope separating the deep ocean from the shelf. Along these, poleward slope currents flow in subsurface; they are observed as far North as Ireland (White and Bowyer, 1997). In the presence of stratification, strong bathymetric gradients trigger in very localized spots the conversion of barotropic tides into internal waves which propagate onto the shelf and into the deep ocean (Pingree et al., 1986). On the continental shelves, intense tidal motions provide the dominant source of energy. The associated turbulent mixing shapes much of the water column properties, preventing under some conditions any surface stratification to setup (Simpson and Hunter, 1974).

Assessment of the Iberia-Biscay-Ireland configuration

C. Maraldi et al.

Title Page

Abstract

Introduction

Conclusions

References

Tables

Figures



Back

Close

Full Screen / Esc

Printer-friendly Version

Interactive Discussion



Assessment of the Iberia-Biscay-Ireland configurationC. Maraldi et al.

[Title Page](#)[Abstract](#)[Introduction](#)[Conclusions](#)[References](#)[Tables](#)[Figures](#)[⏪](#)[⏩](#)[◀](#)[▶](#)[Back](#)[Close](#)[Full Screen / Esc](#)[Printer-friendly Version](#)[Interactive Discussion](#)

From a modelling point of view, this remarkable variety of processes and scales is however particularly challenging. Historically, coastal and deep-ocean numerical models have followed more or less separate paths. The NEMO model (Nucleus for European Modelling of the Ocean; Madec, 2008) used in this study has been developed essentially to perform global, climatic simulations. The recent desire shared by several European operational oceanography centers to hold a single tool for both global and regional applications has strongly influenced its development to that end (O’Dea et al., 2012). It is likely that in turn, global-scale simulations will benefit from more realistic coastal modelling performance. As already explored in other models, explicit representation of tidal motions is likely to become a standard feature of global eddying models in a near future (see Arbic et al., 2010 for instance). Also, one particular aspect in the present model configuration is the relatively high (2–3 km) horizontal resolution used. This clearly pushes the model into the sub-mesoscale permitting regime over much of the domain and allows a significant part of the internal wave spectrum to be resolved.

In this paper, we attempt to give a broad-brush account of one particular aspect of setting up an ocean model, namely consistency verification. This type of validation is often conducted upstream of the implementation of the system which will later be used for production and routinely validated; it is conducted by comparing model results with observations, and is meant to guide model development in identifying gross deficiencies in the modelling of several key physical processes. This is clearly not research, since not much new is learned about the ocean itself, but is an essential task adopting a scientific methodology. Part of the approach adopted in this paper is inspired by past work (e.g. Holt and James, 2001; Holt et al., 2001, 2005; Sotillo et al., 2007), and part follows the specific needs of this work or the availability of data. In particular, a challenging issue is the consistency verification of high-frequency dynamics, such as barotropic and internal tides, or circulation variability at daily time-scales. Besides, we aim at illustrating the potential use of this regional system to provide ocean state estimates which can help interpolate between local or patchy observations and integrate

them in larger-scale patterns and processes. For MyOcean-related reasons, we concentrate on the year 2008.

The paper is organized as follows. Section 2 focuses on the NEMO model, its new developments, and the experimental protocol. Section 3 provides domain-wide consistency verification results in terms of transports, barotropic tides, sea surface temperature (SST) and upper layers stratification. Section 4 focuses on two dynamical sub-regions: the Celtic shelves and the Bay of Biscay slope and deep regions. The model-data consistency is checked for variables and processes such as tidal currents, tidal fronts, internal tides, residual elevation. We also examine the winter warm extension of the Iberian Poleward Current along the northern Spanish coast (Navidad event) in winter 2007–2008. Finally, Sect. 5 gives a summary, a discussion and perspectives for improving the model.

2 Modelling

2.1 NEMO physics and numerical aspects

The IBI model numerical core is based on the NEMO v2.3 Ocean General Circulation Model (Madec et al., 1998; Madec, 2008). It solves the three dimensional primitive equations in spherical coordinates, discretized on an Arakawa C-grid, assuming hydrostatic and Boussinesq approximations. NEMO is written in a generalized vertical coordinate framework allowing some flexibility in the choice of the vertical discretization. Hence, one can easily switch from purely geopotential coordinates (with optionally partial bottom cells as used here) to for instance terrain following vertical coordinates. The bulk of the numerical code used here is very similar to the one described in Barnier et al. (2006). This includes the vector invariant form of the momentum equations and the energy-entropy discretization of vorticity terms. There are however important differences related to the specific coastal and tidal dynamics studied here that are briefly described below.

Assessment of the Iberia-Biscay-Ireland configuration

C. Maraldi et al.

Title Page

Abstract

Introduction

Conclusions

References

Tables

Figures



Back

Close

Full Screen / Esc

Printer-friendly Version

Interactive Discussion



Assessment of the Iberia-Biscay-Ireland configuration

C. Maraldi et al.

Title Page

Abstract

Introduction

Conclusions

References

Tables

Figures

◀

▶

◀

▶

Back

Close

Full Screen / Esc

Printer-friendly Version

Interactive Discussion



In order to properly simulate tidal waves, the default “filtered” free surface formulation (Roullet and Madec, 2000) must be discarded. This scheme has indeed been designed to damp fast external gravity waves in order to extend permissible time step. As an alternative, a conventional time-splitting scheme is used here: the barotropic part of the dynamical equations is integrated explicitly with a short time step (3 s) while the more costly update of depth varying prognostic variables (baroclinic velocities and tracers) is carried out with a larger time step (150 s). The mode coupling procedure as well as the barotropic time stepping scheme (a “generalized forward backward”) follows the work of Shchepetkin and McWilliams (2004) adapted to the standard NEMO leap-frog time stepping of depth varying variables.

Because of the explicit simulations of tides, sea level elevation can become large on the shelf compared to the local depth so that linear free surface approximation needs to be relaxed. In practice, all model vertical thicknesses dz are remapped in the vertical at each time step to account for the varying fluid height according to:

$$dz(x, y, z, t) = dz_0 \left(\frac{H(x, y) + \eta(x, y, t)}{H(x, y)} \right) \quad (1)$$

here dz_0 stands for the vertical “reference” vertical thicknesses, η is the sea level, H is the water depth at rest, (x, y, z) the model geographical coordinates and t the model time step. This vertical coordinate system is called z^* coordinate (Adcroft and Campin, 2004). This implies a correction (here in a standard density Jacobian form) of the hydrostatic pressure gradient force since computational surfaces are not horizontal anymore. The slopes of z^* surfaces remain however small so that the procedure does not give rise to significant errors, and in any case, much lower than with terrain following coordinates.

Vertical turbulent mixing processes are parameterized with a k-epsilon two-equation model implemented in the generic form proposed by Umlauf and Burchard (2002). The model is complemented with the type “A” full equilibrium form of Canuto et al. (2001) stability functions. The turbulent kinetic energy background that accounts

for unresolved internal wave breaking is set to $k_{\min} = 10^{-6} \text{ m}^2 \text{ s}^{-2}$. Dissipation is limited under stable stratification using a Galperin coefficient $c_{\text{galp}} = 0.267$. As discussed by Holt and Umlauf (2008), these two important parameters control the magnitude of the background viscosities/diffusivities away from boundary layers. A part from these, other parameters as well as model equations strictly follow those of Warner et al. (2005) and will not be repeated here. Flux boundary conditions are used for their better accuracy (Burchard et al., 2005). Compared to clamped boundary conditions, Burchard et al. (2005) show that they better handle changes in vertical resolution which is an important requirement here with the highly variable partial bottom cell thicknesses (Fig. 2b). At the bottom a steady balance between shear and dissipation characteristic of log-law behavior is assumed. At the surface, turbulent kinetic injection through surface wave breaking is considered leading to a surface kinetic energy flux (Craig and Banner, 1994):

$$F_{\text{tke}} = \alpha u^{*3} \quad (2)$$

where $\alpha = 100$ is a parameter and u^* the ocean surface friction velocity scale deduced from the wind stress. Related to the wave breaking parameterization is the still largely uncertain choice for the surface roughness zO_s that brings the final piece in the vertical mixing boundary conditions. A common assumption is to scale it with the wind sea wave height H_s so that:

$$zO_s = \gamma H_s \quad (3)$$

γ is a free parameter ranging from 0.6 to 1.6 in the literature ($\gamma = 1.3$ in our case). If no observational nor modelling data are available, various empirical formulae express H_s as a function of wind stress. We followed here the formulation of Raschle et al. (2008)

Assessment of the Iberia-Biscay-Ireland configuration

C. Maraldi et al.

Title Page

Abstract

Introduction

Conclusions

References

Tables

Figures



Back

Close

Full Screen / Esc

Printer-friendly Version

Interactive Discussion



so that:

$$H_s = \frac{\beta}{0.85 g} u^{*2} \quad (4)$$

$$\beta = 665 \left\{ 30 \tanh \left(\frac{w_{\text{ref}}^*}{w^*} \right) \right\}^{1.5} \quad (5)$$

5 where g is the gravity acceleration, w^* the atmospheric friction velocity and $w_{\text{ref}}^* = 0.6 \text{ m s}^{-1}$ a typical wind velocity scale above which wave growth is limited. Raschle et al. (2008) showed that Eq. (4b) better fits their model dataset compared to the classical approach that sets β to a constant value. From the various experiments we made, use of this formulation effectively tapers the effect of wave breaking in case of strong winds
10 which was found to substantially improve the sea surface temperature (comparison with surface buoys).

Along lateral boundaries, free slip boundary conditions are used everywhere except inside Gibraltar strait where no slip conditions are applied. This prevents the Alboran jet in the Mediterranean Sea from turning into an unrealistic quasi-permanent “coastal mode” (i.e. trapped along African coast). At the bottom, a quadratic bottom drag with a logarithmic formulation is calculated as:

$$Cd = \max \left[Cd_{\text{min}} \left\{ \kappa^{-1} \ln \left(\frac{dz_b}{2 z_{0b}} \right) \right\}^{-2} \right] \quad (6)$$

where $\kappa = 0.4$ is the Von Karman constant, $Cd_{\text{min}} = 2.5 \times 10^{-3}$ a minimum drag coefficient, dz_b is the lowermost bottom cell thickness and $z_{0b} = 3.5 \times 10^{-3} \text{ m}$, the bottom roughness. With the reference geopotential discretization chosen here, the logarithmic formulation applies for depths shallower than 170 m, i.e. on most of the continental shelf
20 (Fig. 2c). Although ocean models interchangeably assume constant or logarithmic formulations as bottom drag formulation, the use of Eq. (5) is mandatory here to ensure a

continuous (i.e. not related to numerical settings such as the vertical discretization) representation of bottom stress as it should be in nature. This somewhat counterintuitive property owing to the largely spatially discontinuous drag coefficient (Fig. 2c), comes from the tight interplay between the modeled vertical shear and the vertical mixing scheme (impact on model stability of this interplay was further evidenced by Burchard et al., 2005). The formulation of the bottom stress must agree with the assumed law of the wall in the vertical mixing scheme, a requirement emphasized here by the use of partial bottom cells.

Tracers' advection is computed with the QUICKEST scheme developed by Leonard (1979). This 3rd order scheme is well suited to the high resolution used here and the modelling of the sharp front characteristics of coastal environments. Lateral sub-grid scale mixing are parameterized according to horizontal biharmonic operators for both momentum ($A_m = -2.5 \times 10^8 \text{ m}^4 \text{ s}^{-1}$) and tracers ($A_t = -2.5 \times 10^7 \text{ m}^4 \text{ s}^{-1}$). Note that the latter value is particularly small, since significant inherent diffusion is also associated with the QUICKEST scheme.

2.2 Model setup

The model domain covers the North East Atlantic ocean from the Canary Islands to Iceland and from about 20° W to 10° E (Fig. 1). Even if the focus of the IBI forecasting system remains on the Iberian, Biscay, and Irish regions, the computational domain has been extended to include the Western Mediterranean Sea and the North Sea. This strategy has been chosen to lessen the impact of Northern and Eastern boundaries with the parent model, PSY2V3. Indeed the PSY2V3 model, an operational forecasting system covering the North Atlantic and the Mediterranean Sea with a $1/12^\circ$ resolution, does not simulate all the physical processes of interest here (tides in particular). Moreover, such strategy allows for the explicit computation of mass, heat and salt fluxes in the narrow Gibraltar and Kattegat straits which we expect will be better resolved thanks to the improved horizontal resolution.

Assessment of the Iberia-Biscay-Ireland configuration

C. Maraldi et al.

Title Page

Abstract

Introduction

Conclusions

References

Tables

Figures



Back

Close

Full Screen / Esc

Printer-friendly Version

Interactive Discussion



Sea was highly dependent on the chosen H_{\min} value if simply set, for instance, to a uniform value greater than the maximum tidal amplitude in the area (≈ 10 m). We finally set:

$$H_{\min}(x, y) = \max[5 \text{ m}, 1.2 \text{ Atide}_{\max}(x, y)] \quad (7)$$

5 where $\text{Atide}_{\max}(x, y)$ is the maximum tidal amplitude (we use here as a rough estimate the sum of FES2004 elevation amplitude harmonics (see Lyard et al., 2006, for a description of the FES2004 tidal atlas).

2.3 Forcing

2.3.1 Atmospheric forcing

10 Meteorological fields from the European Centre for Medium-Range Weather Forecasts (ECMWF) with a 3-h period and 0.25° horizontal resolution drive the present model simulations. According to Bernie et al. (2005), this temporal resolution associated with adequate vertical resolution in surface layers (typically one meter as used here or less) is sufficient to model diurnal variations of SST. Evaporation, latent and sensible heat fluxes and wind stresses are computed according to Large and Yeager (2004) bulk
15 formulae. Net longwave heat flux is obtained from ECMWF downward flux to which the following blackbody radiation is added:

$$Q_{\text{bb}} = -E\sigma(\text{SST} + 273.15)^4 \quad (8)$$

where σ is the Stefan-Boltzman constant and $E = 0.99$, the emissivity.

20 Penetrative solar radiation Q_{sr} is parameterized according to a two band exponential scheme such that:

$$Q_{\text{sr}}(z) = Q_{\text{sr}}(0) \left\{ R e^{-z/l} + (1 - R) \text{pt} e^{-z k_{\text{PAR}}} \right\} \quad (9)$$

The first exponential term from the left corresponds to red and near infrared radiation absorbed in surface layers (the chosen e-folding length scale is $l = 0.35$ m) while the

Title Page

Abstract

Introduction

Conclusions

References

Tables

Figures

◀

▶

◀

▶

Back

Close

Full Screen / Esc

Printer-friendly Version

Interactive Discussion



Assessment of the Iberia-Biscay-Ireland configuration

C. Maraldi et al.

Title Page

Abstract

Introduction

Conclusions

References

Tables

Figures

◀

▶

◀

▶

Back

Close

Full Screen / Esc

Printer-friendly Version

Interactive Discussion



second refers to shorter wavelengths mostly in visible and ultraviolet bands. $R = 0.54$ determines the fraction in each band of the available penetrative solar radiation at the surface $Q_{sr}(0)$ (we assume a constant albedo of 6.6 %). The latter part of the spectrum penetrates at much greater depths and participates to photosynthesis so that it is often referred to as photosynthetically attenuation radiation (PAR). While there is little variation of absorption depth in the first band, PAR absorption coefficient (k_{PAR}) is highly dependent on ocean turbidity. Since the IBI model domain encompasses areas with very different optical water properties (from highly turbid on the shelf to clear waters in the subtropical gyre, see Fig. 2a), a spatially variable k_{PAR} coefficient has been used. It is built from a 10 yr, 9 km, monthly climatology of Seawifs satellite diffusive attenuation coefficient at 490 nm (kd_{490}), transformed into an equivalent PAR attenuation coefficient according to Morel et al. (2007):

$$k_{PAR} = 0.0665 + 0.874kd - 0.00121 \frac{1}{kd_{490}} \quad (10)$$

Equation (9) and the different algorithms used for the retrieval of attenuation from satellite data are nevertheless only valid for Case-1 waters (where chlorophyll concentration controls optical properties). As a correction, Seawifs based estimate is merged with a monthly climatology processed by Ifremer (Gohin et al., 2005) which is valid in coastal waters. The k_{PAR} threshold value between Case-1 and Case-2 waters (over which Ifremer data only is considered) has been set to 0.12 m^{-1} . This value is more or less the lower bound of agreement of Gohin et al. (2005) estimate if compared to in situ measurements.

2.3.2 River runoffs

At 33 major rivers mouths (shown in Fig. 2a), climatological monthly flow-rates are prescribed. These have been obtained by averaging data from the Global Runoff Data Center (<http://grdc.bafg.de>) and the French hydrographic database “Banque Hydro” (<http://hydro.eaufrance.fr>). Rivers are applied by specifying (i) a constant velocity in

the vertical whose integral matches the specified transport, (ii) Neumann condition for temperature and (iii) a constant salinity (0.1 PSU).

2.3.3 Open boundaries

After numerous tests, relatively simple, yet robust open boundary formulations have been chosen. The method of characteristics is used for barotropic variables following Blayo and Debreu (2005). These conditions are expressed as (for a western open boundary):

$$\bar{U}b = \frac{1}{2} \left(\bar{U}_i + \bar{U}_{\text{ext}} + \sqrt{\frac{g}{h}} (\eta_i - \eta_{\text{ext}}) \right)$$
$$\bar{V}b = \bar{V}_{\text{ext}} \text{ if } \bar{U}_{\text{ext}} > 0 \text{ else } \bar{V}b = \bar{V}_i \quad (11)$$

where \bar{U} and \bar{V} refer respectively to normal and tangential barotropic velocities; g is the gravity acceleration, h the water depth and η the sea level. Index b corresponds to the prescribed boundary value, index i to the model computed value immediately inside the domain and index ext to external data. A Neumann condition for elevation is used while baroclinic velocities, temperature and salinity are prescribed to external data. For the latter variables a 30-points relaxation area with a minimum time-scale of 1 day is used which strongly damps outgoing perturbations from the prescribed fields while allowing for the explicit simulation of high frequency fluctuations related to the atmosphere in the surface layers.

Temperature, salinity, velocities and sea surface height (hereafter SSH) from PSY2V3 daily outputs are used as the slow component of open boundary data. PSY2V3 does include a multivariate, Kalman based, weekly data assimilation procedure of along track altimetry data, SST and hydrological observations (Dréville et al., 2008; Dombrowsky et al., 2009). SSH and barotropic velocities tidal components are then added as the sum of a maximum of 11 constituents (M2, S2, K2, N2, K1, O1, P1, Q1, M4, Mf, Mm) provided by the TPXO 7.1 global tide model (Egbert et al., 1994).

Assessment of the Iberia-Biscay-Ireland configuration

C. Maraldi et al.

Title Page

Abstract

Introduction

Conclusions

References

Tables

Figures

◀

▶

◀

▶

Back

Close

Full Screen / Esc

Printer-friendly Version

Interactive Discussion



**Assessment of the
Iberia-Biscay-Ireland
configuration**C. Maraldi et al.

[Title Page](#)[Abstract](#)[Introduction](#)[Conclusions](#)[References](#)[Tables](#)[Figures](#)[Back](#)[Close](#)[Full Screen / Esc](#)[Printer-friendly Version](#)[Interactive Discussion](#)

A 35-day barotropic experiment, (i.e. without stratification) with clamped boundary conditions for sea level and Neumann conditions for velocities, is computed to estimate the 6 major barotropic tidal velocities constituents used for the open boundary conditions (similar to the runbt experiment described below). This method, reminiscent of the iterative procedure of Flather (1987), clearly improved the overall tidal statistics (semidiurnal phases otherwise exhibit significant errors due to the inadequacy of TPXO velocities with the model physics).

Finally, since surface atmospheric pressure forcing is explicitly considered in the dynamical equations, the inverse barometer signal (IB) is added to sea level open boundary data. In the Atlantic part of the domain, IB is a fairly good approximation of the sea level response to pressure variations while it has serious limitations in a semi-enclosed sea like the Mediterranean Sea (Le Traon and Gauzelin, 1997). Since we essentially focus on the Atlantic side of the basin, we have left for further study the use of more sophisticated methods (such as Candela, 1991 analytical model in the Mediterranean Sea) or outputs from Baltic and Med Sea models that do explicitly include the pressure component. As demonstrated in the following, this simplification still allows for pretty realistic variations of Mediterranean outflow transport at Gibraltar, which can be considered as the boundary of our domain of interest.

2.4 Experiments

Results from two simulations will be considered in the next sections:

1. A “tide only” run (hereafter runbt) which consists in a 35-day “barotropic-like” simulation (homogenous density, no atmospheric forcing, only tidal forcing). Since proper representation of bottom boundary layers is also of interest here, this experiment retains the 50 vertical levels distribution and the k-epsilon vertical mixing scheme described above. Compared to realistic simulations, it will provide insights on the impact of stratification, and, in particular, changes due to internal waves on the simulation of tidal waves. Note that a reduced set of 7 harmonics (M2, S2,

Assessment of the Iberia-Biscay-Ireland configuration

C. Maraldi et al.

Title Page

Abstract

Introduction

Conclusions

References

Tables

Figures

◀

▶

◀

▶

Back

Close

Full Screen / Esc

Printer-friendly Version

Interactive Discussion



N2, K1, O1, Q1, M4) is used since these waves are separable through harmonic analysis over such a short simulation period. Since these harmonics represent most of the tidal energy, it is expected that this will not hamper the comparison to the realistic experiment.

2. A realistic simulation with full forcing and stratification (hereafter runbc). It has been initialized on July 25th, 2007 from temperature, salinity, sea level and velocities linearly interpolated from PSY2V3 analysis. Tidal and atmospheric pressure forcing are smoothly introduced (both at open boundaries and in dynamical equations) thanks to a 2 day linear ramp. Meanwhile, horizontal viscosity linearly decreases from 4 times its nominal value, to damp instabilities arising from the use of unbalanced initial fields. The simulation ends in February 2009. In the next sections, we focus on year 2008 only.

3 General assessment

3.1 Barotropic tides

3.1.1 General comments

Since tidal motions are the dominant source of energy on the continental shelf, we give here some quantitative assessment of model performance on that particular aspect. Numerous modelling studies have already conducted such an exercise (Davies and Aldridge, 1993; Davies et al., 1997; Holt and James, 2001), which has proven to be sensitive to various numerical details, due in particular to the complex tidal propagation pattern in the English Channel and the North Sea. In order to keep the present account synthetic enough, a detailed description of the different tests performed to reach the present results cannot be given. The use of “equilibrated” boundary conditions as described in Sect. 2.3.3 is obviously one of the keys as well as the use of the tide-generating force owing to the size of the domain.

Assessment of the Iberia-Biscay-Ireland configuration

C. Maraldi et al.

Title Page

Abstract

Introduction

Conclusions

References

Tables

Figures

◀

▶

◀

▶

Back

Close

Full Screen / Esc

Printer-friendly Version

Interactive Discussion



Here we solve this problem with the use of geopotential coordinates. Terrain-following coordinates have historically been preferred to maintain sufficient vertical resolution at the bottom and to have a continuous representation of the bathymetry. The use of partial bottom cells nevertheless partially restores the latter property with z-coordinates.

Moreover, the vertical discretization chosen here sets the level of the last wet cell at most at 10 m above the bottom for depths lower than 150 m (Fig. 2b), which should be enough to properly resolve the bottom boundary layer.

An aspect that also deserves some attention is the impact of stratification on tidal amplitudes. The high resolution used here is expected to allow a significant part of the tidally induced internal wave spectrum to be resolved, which in turn provides an important sink of energy for barotropic tides. In forward global tide modelling, correctly accounting for this barotropic to baroclinic conversion explicitly or through ad-hoc parameterizations has now become a key for further improvement (Arbic et al., 2010; Lyard et al., 2006). In the next paragraphs, we examine results of a 1-yr harmonic analysis on the runbc experiment. These are eventually compared to the barotropic experiment runbt with harmonic analysis performed over the last 30 days.

3.1.2 Tidal elevations

The M2 co-tidal chart is shown in Fig. 3a and depicts the complex wave propagation around amphidromes in the North Sea. The overall picture is in good agreement with published charts, including the position of the degenerate amphidrome south of Norway that has proven to be difficult to obtain in other modelling studies (O'Dea et al., 2012). Further insights of the model performance can be gained by comparing the result to FES2004 atlases (Lyard et al., 2006). The FES2004 solution has been obtained through the use of a finite-element hydrodynamical model assimilating altimetry and in-situ harmonic data; it can be considered a fairly reliable reference at least in the deep ocean. Figure 3b shows M2 difference with the FES2004 solution, amplitudes differences being generally smaller than 1 cm in the deep ocean ($z > 1000$ m), phase errors (not shown) being negligible. Most of the differences there are related to the

surface signature of internal waves which are further investigated in Sect. 4.3.2. On the shelf, the regional model is close to the FES2004 solution, except in the Dover Strait area and in the German Bight. From the same comparison performed in the barotropic experiment, it is interesting to note that much larger differences arise when no stratification effects are present (Fig. 3c). The M2 wave amplitude in that case is systematically overestimated, a difference reaching more than 15 cm at the western Channel entrance and in the Irish Sea (phase is not significantly different between experiments). From the pattern of the amplitude difference between experiments (not shown), it is tempting to relate this difference to barotropic to baroclinic energy transfer: wave amplitude indeed undergoes a sharp decrease at 48° N along a well observed spot of internal wave generation. Since other factors may explain the differences between experiments (effect of stratification on viscosity profiles for instance), a separate study beyond the present “global” assessment would however be needed to firmly reach that conclusion.

To gain some more quantitative measure of errors, comparisons are made at various tide gauge locations for the four main tidal constituents (M_2 , S_2 , K_1 , O_1). Comparison for M_4 compound wave is also considered, as an indicator of how well non-linear interactions are modelled, in particular those induced by the z^* coordinate (Eq. 1). For each tidal component, the RMS of the complex difference (see Davies et al., 1997 for the definition), which synthesizes both amplitude and phase errors, is given in Table 1. To appreciate how significant these errors are, it is instructive to make a comparison with modelling studies based on well validated shelf sea models such as the *POLCOMS* model used in Holt et al. (2001, 2005). Considering the overlapping area between both models, the present experiment has similar accuracy for M2 (21.6 cm against 24.1 cm in IBI). IBI has larger errors for the M_4 component, but it seems to outperform the Holt et al. (2005) model on the other components, with errors reduced by more than a half for the diurnal component. We however stress that measurement points differ between our study and Holt et al., the present dataset being essentially distributed along the coast.

Assessment of the Iberia-Biscay-Ireland configuration

C. Maraldi et al.

Title Page

Abstract

Introduction

Conclusions

References

Tables

Figures

◀

▶

◀

▶

Back

Close

Full Screen / Esc

Printer-friendly Version

Interactive Discussion



3.1.3 Barotropic tidal currents

Only a brief account is given here on barotropic tidal velocities since a more detailed discussion on total surface tidal currents is given in the regional assessment section. Table 2 gathers comparisons to in-situ observations shown in Fig. 4 for the dominant M2 tidal component in the runbt simulation. The overall agreement is rather good with a global RMS error of 4.5 cm s^{-1} for the semi-major axis, model velocities being generally slightly larger than observations. Along the shelf slope in the northern part of the Bay of Biscay, where lots of measurement are available, absolute errors are smaller than 8 cm s^{-1} (75% are smaller than 4 cm s^{-1}). This is of similar accuracy than in the regional model of Pairaud et al. (2010). Results with full forcing and stratification exhibit very similar errors (RMS= 3.8 cm s^{-1}), velocities being however slightly underestimated.

3.2 Large-scale circulation

3.2.1 Transports

Transport estimates give access to broad lines of the model circulation. Monthly volume, heat and freshwater transports are computed across various sections and are compared to previous published estimates (Table 3). Note that published transport values from observations do not always contain transport error estimates. The standard deviation of published estimates from the monthly model transports is used to give an order of magnitude of the errors between model and observations (Table 3). This value includes model errors as well as transport interannual variability.

For Sect. 1, the transports associated with the Azores Current and the Mediterranean Water (MW) outflow (15.1 Sv and -12.3 Sv) are larger than the eastward and westward observed transports of 13.7 Sv and -4.7 Sv (Peliz et al., 2007). However the observed estimates are deduced from data obtained in September–October of two consecutive years in 1991 and 1992 and the modelled estimates show high monthly variability

Title Page

Abstract

Introduction

Conclusions

References

Tables

Figures

⏪

⏩

◀

▶

Back

Close

Full Screen / Esc

Printer-friendly Version

Interactive Discussion



indicating that the eastward flow is of comparable magnitude with observations while the westward flow is overestimated.

Across the Gibraltar Strait, model transports have been computed from monthly averaged values of currents and salinity (Atlantic Water inflow of 0.48 Sv and the MW outflow of -0.49 Sv). Tsimplis and Bryden (2000) found values of 0.46 Sv and -0.35 Sv at the Gibraltar Strait using currents averaged over several months (estimations not included in Table 3). However the flow variability is dominated by high frequency tidal currents through the Strait of Gibraltar (Tsimplis and Bryden, 2000) and transports across the Gibraltar Strait are commonly computed from hourly or daily fields rather than from yearly averaged salinity and velocity fields. Using this method, we obtain transports of 0.51 Sv in the upper layer and of -0.71 Sv in the lower layer which lie within the range of observation based estimates. We also note that the outflow is larger than the inflow while the inflow is normally larger to compensate the excess of evaporation minus precipitation over the Mediterranean Sea. In the IBI solution, the outflow transport is mainly influenced by the open boundary conditions prescribed from the PSY2V3 solution which explains the larger outflow in the strait.

In the Gulf of Cadiz the modelled transports (1.77 Sv/ -0.04 Sv) are very small compared to published values (3.1 Sv/ -2.8 Sv; Mauritzen et al., 2001). Previous estimates use a density of 31.7 to separate inflow of Atlantic Water from outflow of MW but comparisons of hydrological fields with climatology have shown that the MW is too light in the model (not shown) and the 31.7 isodensity may not be appropriate to separate the two water masses. When choosing a density threshold value of 30.3 in the Gulf of Cadiz region, we obtain transports of 2.0 Sv and -1.1 Sv across the Gulf of Cadiz and a transport of -1.3 Sv for the MW. The results are closer to the estimates from observations and the transport lies within the range of published values for the inflow but the westward flow is still underestimated (Howe, 1984; Rhein and Hinrichsen, 1993; Mauritzen et al., 2001). South of Portugal, the MW flows northward with a transport comparable with previous estimations (Jorge da Silva, 1996; Mazé et al., 1997; Coelho et al., 2002). Off West Iberian Peninsula the transport is slightly overestimated at 40° N

Assessment of the Iberia-Biscay-Ireland configuration

C. Maraldi et al.

Title Page

Abstract

Introduction

Conclusions

References

Tables

Figures



Back

Close

Full Screen / Esc

Printer-friendly Version

Interactive Discussion



but is in good agreement with previous estimates at 43° N (Sect. 6 and 7; Jorge da Silva, 1996; Mazé et al., 1997; Mauritzen et al., 2001; Coelho et al., 2002; Alvarez et al., 2004; Lherminier et al., 2007).

5 Transports of the slope current across the Celtic shelf slope and along the Ellett line are of the same order of magnitudes than published values (Ellett and Martin, 1973; Pingree and Le Cann, 1990; Holliday et al., 2000). However we note that the transport across the Celtic slope is mainly constrained within the upper slope in the model while it is more evenly distributed along the slope in the study of Pingree and Le Cann (1990).
10 The distribution of the transport with depth is comparable with estimations from data across the Ellett line section. Through the Dover Strait observed and modelled are both very weak (Otto et al., 1990; Prandle et al., 1996) but the transport is slightly underestimated in IBI.

3.2.2 Mediterranean outflow

15 The transport through the Strait of Gibraltar is controlled by various processes at different time scales. Among these processes, tides are the most energetic one influencing the mean flow (Tsimplis and Bryden, 2000). Thus hourly transport through the Gibraltar Strait has been calculated to examine the outflow variability. Following the study of Sánchez Román et al. (2009) the interface to separate the inflow from the outflow has been defined as the time dependent depth of the surface of zero low-pass frequency
20 velocity. The modelled outflow transport estimated with this interface is noted TMV (Transport Model Velocity). The outflow transport computed using the commonly used 37.25 isohaline (TMS, Model Salinity) is also computed for comparisons. Figure 5 illustrates time series of observed and modelled transports for TMV and TMS over a period overlapping the model simulation and the transport estimates of Sánchez Román et al. (2009), noted TOV (Observation Velocity). The definition of the interface based on
25 the depth of the zero velocity gives better results than the isohaline interface. In comparison to the TOV mean transport of -0.72 Sv, the mean outflow of TMV is -0.74 Sv and the correlation coefficient with TOV is 0.71, while a lesser agreement is found for

Assessment of the Iberia-Biscay-Ireland configuration

C. Maraldi et al.

Title Page

Abstract

Introduction

Conclusions

References

Tables

Figures



Back

Close

Full Screen / Esc

Printer-friendly Version

Interactive Discussion



TMS with a too small transport of -0.69 Sv and a correlation coefficient of 0.66. Differences between peak values and lower values at neap tides reach 0.70 Sv both in TOV and TMV.

3.3 Sea surface temperature

3.3.1 SST datasets

We use SST processed at Météo-France/CMS for comparisons with the model SST (Le Borgne et al., 2011). Data consist in L3 multi-sensors products built from bias-corrected L3 mono-sensor products. SST satellite data fields are produced daily with a 0.05° resolution and an accuracy of 0.5°C . Sea surface temperature measured from in situ buoys is also used (Fig. 1, Table 4). The dataset consists in hourly time series which enable the computation of the diurnal cycle.

3.3.2 Daily to seasonal SST variability

Figure 6a represents maps of seasonal SST biases and RMS of differences between the satellite data and the model fields, for summer (July-August-September) and winter (January-February-March). The mean bias over the whole IBI area is low (less than 0.25°C) over the whole year but is not evenly distributed in space and time. In winter, the bias is lower than 0.2°C and the RMS of the difference is on average below 0.5°C . Discrepancies are higher in summer, with biases locally larger than 1°C over the Armorican shelf, in the English Channel and west of Iberia. West of Iberia the model is too warm in both seasons with the SST overestimation being larger in summer during upwelling season. In the Irish Sea, at the entrance of the English Channel and in the Iroise Sea, the discrepancies of $1-1.5^\circ\text{C}$ may be explained by the high variability of thermal frontal positions which are tidally induced as discussed in Sect. 4.2. In the Gulf of Cadiz (GC) the modelled SST is too warm along the slope, which reveals the model's relative failure at representing the GC slope current (GCC). The GCC, intimately linked

Title Page

Abstract

Introduction

Conclusions

References

Tables

Figures

⏪

⏩

◀

▶

Back

Close

Full Screen / Esc

Printer-friendly Version

Interactive Discussion



to the westward MW outflow at depth (Peliz et al., 2009), indeed advects cold upwelled water along the western Portuguese coast into the GC. This stresses the model's limits, already outlined above, at representing MW outflow in its present version.

Figure 7 represents a Taylor diagram of the observed and modelled SST at buoy locations (Fig. 1, Table 4). SST time series have been previously 1-day low pass filtered to remove the diurnal cycle signal which is discussed in the next section. SST is particularly well modelled in IBI with “normalized” standard deviation close to 1 and correlation greater than 0.95 (except at Cabo Silliero and Villano Sisargas where the correlation coefficients are 0.85 and 0.89, respectively). When looking regionally, larger discrepancies are found along the Armorican slope and within the Gulf of Cadiz, due to overestimated modelled SST during summer. Warmer model SST during summer at these locations leads to a larger seasonal amplitude.

The IBI model ability to reproduce the SST variability results from the high spatial resolution and from model developments (see Sect. 2); the latter allow the model to simulate and predict slope and shelf processes (e.g. tidal mixing) better than deep ocean configurations such as PSY2V3 (however SST data assimilation leads to realistic SST simulated fields in PSY2V3). The model-data discrepancies in the upwelling areas suggest to investigate the sensitivity of the model response in these areas to the wind product used to force the model.

3.3.3 Diurnal SST cycle

The combination of daily variations of atmospheric fluxes and weak winds can lead to strong SST diurnal anomalies (hereafter Dsst). The Dsst amplitudes are computed over a 24-h period as the difference between the maximum SST and the minimum SST previously corrected from the daily trend (Pimentel et al., 2008). The Dsst for the buoy data are only computed when the 24 SST values per day are available to avoid any miscalculations of the Dsst amplitudes.

Figure 7 displays box plots of the observed and the modelled Dsst amplitudes over the Bay of Biscay, the Celtic Shelves and the North Sea (areas shown in Fig. 3); it

Assessment of the Iberia-Biscay-Ireland configuration

C. Maraldi et al.

Title Page

Abstract

Introduction

Conclusions

References

Tables

Figures



Back

Close

Full Screen / Esc

Printer-friendly Version

Interactive Discussion



illustrates the distribution of data by showing different values of Dsst amplitudes below which a certain percentage of data are observed. Globally Dsst amplitudes are underestimated in the model and the median observed Dsst is 0.25°C while the median modelled Dsst is only 0.20°C . When looking regionally at the distribution, we found that Dsst is underestimated almost everywhere for the 50 % of the data with smaller amplitudes (i.e. Dsst amplitudes below the median value). The resolution of the model and of the forcing, the surface heat fluxes and the vertical mixing in the upper ocean are critical aspects for the diurnal cycle modelling (Pimentel et al., 2008). According to Bernie et al. (2005), a minimum of a 1 m vertical resolution in the upper ocean and of a 3-h temporal resolution of surface fluxes is required to simulate 90 % of the observed Dsst. IBI is forced with 3-h atmospheric fields but has a coarser vertical resolution with 8 levels (respectively 18 levels) in the top 10 m (resp. 50 m) that enables to only represent 70 % of the Dsst (Bernie et al., 2005). This partly explains the underestimation of the Dsst in the model. Overestimated wind stress may also lead to an underestimation of the Dsst by inducing too strong vertical turbulent mixing and preventing from diurnal heating. As for lower frequencies (see previous section), we recommend further assessment on the realism of the wind field forcing.

3.4 Upper layers stratification

The upper layers stratification is a key process to represent in a regional model for its implications on circulation and energetics, in particular at the air-sea interface, and for its strong influence, or even coupling, with biological processes. The subsurface ocean is sparsely sampled with observations. In the Bay of Biscay for instance, only two moorings of hourly temperature and salinity (*T/S*) profiles are available to the community (see Sect. 4.3.3). UK MetOffice provides the so-called EN3 dataset that gathers subsurface *T/S* profiles from different sensors (e.g. ARGO floats) with quality control based on a comprehensive set of checks (Ingleby and Huddleston, 2007). Figure 8 illustrates the available data for February and August 2008 (only profiles at least 200 m deep are used). The sampling is inadequate for a detailed investigation of the processes

Assessment of the Iberia-Biscay-Ireland configuration

C. Maraldi et al.

Title Page

Abstract

Introduction

Conclusions

References

Tables

Figures



Back

Close

Full Screen / Esc

Printer-friendly Version

Interactive Discussion



underlying the T/S distribution. Instead it allows an overall view of the model performance in different areas.

Figure 8 shows the RMS of the model-data misfits in temperature over the upper 200 m. We also compute the mixed layer depth (MLD) from the model and EN3 profiles using a criterion on density and a threshold of 0.02 kg m^{-3} (not shown). In February, modelled temperatures show very good agreement with data almost everywhere with RMS globally lower than 0.5°C . The profile of temperature RMS computed over the whole IBI domain (not shown) indicates that maximum RMS values are reached between 50 m and 130 m which is consistent with differences in modelled and observed MLD at these depth ranges. In August, larger RMS in temperature profiles (up to 2°C) are found on shelves as well as in the deep ocean, with a model overestimation of the temperature in the upper 200 m, in the Iroise Sea and in the English Channel. The MLD is underestimated in the model in summer.

Besides the difficulty of single point comparison (in particular because of the mesoscale signals), these comparisons emphasize the need to further test the vertical mixing physics: parameterization and values of parameters, as well as forcing fields (impact of over- or underestimation of wind forcing on turbulence). Another possible source of error may be the wave mixing parameterization coefficient. Sensitivity experiments performed with a $1/12^\circ$ resolution configuration have shown that the modelled MLD (and consequently temperatures in the upper ocean layers) is very sensitive to the wave mixing parameterization coefficient. The model MLD representation can be enhanced by tuning this parameter but the parameterization seems to be inadequate in semi-enclosed seas as the Mediterranean Sea or the North Sea. Thus the parameter used is a compromise to minimize the MLD errors both in the open ocean and in the semi-enclosed seas.

Assessment of the Iberia-Biscay-Ireland configuration

C. Maraldi et al.

Title Page

Abstract

Introduction

Conclusions

References

Tables

Figures



Back

Close

Full Screen / Esc

Printer-friendly Version

Interactive Discussion



4 Regional skill assessment

4.1 Introduction

We now focus on the Bay of Biscay and explore the model-data consistency for processes specific to the shelf (Sect. 4.2) and slope and deep regions (Sect. 4.3). The surface circulation in the Bay of Biscay is relatively weak over the abyssal plain (a few cm s^{-1} , Charria et al., 2011); it is mainly cyclonic in winter and anticyclonic in summer. Slope currents have been evidenced off the northern Iberian coast and over the Armorican shelf break (Pingree and Le Cann, 1990), with significant time variability (see Sect. 4.3.5 for the Iberian Poleward Current). The circulation over the shelves is dominated by tidal currents; the residual currents are mostly wind-driven and are highly variable in time. Anticyclonic and cyclonic eddies are observed in the deep region; they mostly result from instabilities of the slope current developing at capes and canyons (Pingree and Le Cann, 1992). Internal tides are generated in regions of interaction between barotropic tidal currents and the shelf break. Two sites of generation have been described in the literature: the Armorican Shelf break around 47°N (Pairaud et al., 2010) and the Galician coast (Pichon and Corréard, 2006).

We investigate the representation of these processes based upon the available observations. The emphasis is on shelves and slopes because of potential implication for users in biology or other downstream applications of the IBI system. We also examine the representation of the Iberian Poleward current flow along the northern Spanish coasts in winter. The objective is to show that such a regional modelling system has potential as a complement to observations (an integrated approach) to give information on non-observed physical quantities and to provide links between observations.

OSD

10, 83–151, 2013

Assessment of the Iberia-Biscay-Ireland configuration

C. Maraldi et al.

Title Page

Abstract

Introduction

Conclusions

References

Tables

Figures



Back

Close

Full Screen / Esc

Printer-friendly Version

Interactive Discussion



ad hoc studies will be required in order to better identify the source of the discrepancies whenever applications will require good estimates of tidal currents.

4.2.2 Tidal fronts

The occurrence of thermal fronts due to tidal mixing is a common feature on the European continental shelf. Thermal fronts appear in summer when tidal mixing prevents surface stratification from solar insolation to set up. They separate tidally mixed waters from stratified waters. Following the study of Holt et al. (2008), we estimate the capability of the model in reproducing the location of tidal mixing fronts by comparisons with mean frontal positions as estimated from climatological ICES data (<http://www.ices.dk/>). We perform a similar analysis over 2008: data consist in ICES temperature profiles covering the June-August period and mean tidal fronts are deduced from the observed surface to bottom difference defined by $\Delta T = 0.5^\circ\text{C}$. The same approach is applied to model temperature profiles. Results are presented in Fig. 10. Over the shelf, SST fronts are due to the vertical turbulent mixing generated by tidal stresses at the seabed; the model shows reasonable agreement with observations in the main tidal front positions over the shelf, particularly for the Ushant front (north-west coast of Brittany), at the entrance of the English Channel, in the northern Irish Sea, off North Scotland and south of Doggar Bank (along $\sim 54^\circ\text{N}$). MODIS SST data have also been used to perform qualitative comparisons of the SST fronts (Fig. 11). The modelled SST shows a very good agreement with observations in the main tidal front positions. Over the shelf, the model presents larger stratified regions in the Irish Sea and colder SST in the Ushant front (Off West Brittany) and at the entrance of the English Channel. Elsewhere SST fronts are relatively well represented both in temperature and in extension. On the Armorican shelf break, internal tides induce strong vertical mixing which prevents from the formation of seasonal stratification and results in a cold SST tongue along the shelf break from 11°W to 5°W . The cold intrusion is also reproduced in the model: temperature is underestimated by 0.5°C and the south-eastward extension is relatively well represented. The relatively good accuracy of the

Assessment of the Iberia-Biscay-Ireland configuration

C. Maraldi et al.

Title Page

Abstract

Introduction

Conclusions

References

Tables

Figures



Back

Close

Full Screen / Esc

Printer-friendly Version

Interactive Discussion



model in reproducing these tidal mixing fronts is mainly related to the good representation of the bottom stress which affects the propagation of barotropic tidal waves, the k-epsilon two-equation model combined with the closure model of Canuto et al., (2001), the limitation of the dissipation under stable stratification and the tracers advection (Holt et al., 2008). Model presents weaker stratification over Doggar Bank and West of England, and summer stratification is overestimated in the southern Irish Sea. Differences with observed mean frontal positions are also seen southwest of Denmark. Salinity stratification is important in this region (two major rivers including the Elbe river) and may impact frontal position (Holt et al., 2008).

4.2.3 Surges

For verification purposes, we diagnose the model ability to reproduce surges by comparing residual elevations (i.e. detided sea levels) from the model with in situ measurements at time scales shorter than 10 days. At these time scales, the simulated coastal sea level is the signature of the static and non static response to atmospheric pressure, of the response to wind forcing and of tidal interactions (see for instance Carrère and Lyard, 2003). The in situ sea level dataset consists in 115 tide gauges located along the European coasts (see red dots on Fig. 1). The harmonic analysis tool from Puertos del Estado is used to compute the tidal component from tide gauge elevations and to predict the tidal elevations; this software was developed to be used within the ENSURF ensemble system (Pérez et al., 2012) and is based on the Foreman harmonic analysis (Foreman, 1977).

Comparisons between residual elevations from the model and the observations are shown in Fig. 12 for the Bay of Biscay and the English Channel. The elevations due to the static response of the ocean to atmospheric pressure (the so-called Inverse Barometer or IB effect) alone have been included in the comparison. The model shows very good agreement with data (90 %, respectively 67 %, with RMS difference smaller than 5 cm, respectively 3 cm, and 80 % with correlation greater than 0.9) and it performs better than the IB response (54 % with RMS difference smaller than 5 cm). It is most

Assessment of the Iberia-Biscay-Ireland configuration

C. Maraldi et al.

Title Page

Abstract

Introduction

Conclusions

References

Tables

Figures



Back

Close

Full Screen / Esc

Printer-friendly Version

Interactive Discussion



effective at high latitudes which are more energetic areas and where the ocean dynamical space and time scales are smaller, while at mid latitudes the model response to atmospheric forcing is closer to the IB approximation (not shown).

4.3 IBI shelf breaks and deep ocean

4.3.1 Surface tidal currents over the slope

Surface tidal currents from runbc are compared to observed currents at buoy stations along the northern Iberian coast for the M2 constituent (Fig. 9c). The model tends to overestimate the current amplitudes almost everywhere. The largest differences are found at Villano Sisargas: the modelled ellipse azimuth is remarkably consistent with the observations, but the modeled semi major axis is more than twice as large as the observed one. García-Lafuente et al. (2006) also found the M2 barotropic tidal currents were much greater than expected in this area; they attributed it to internal tides of considerable amplitudes. Pichon and Corréard (2006) showed that the northwest Spanish continental slope is indeed an area of internal tide generation. In the vicinity of Villano Sisargas differences of the M2 surface current amplitudes between the run with stratification (runbc) and the run without stratification (runbt) present high values due to internal tides (Fig. 9c). As internal tides generation is very sensitive to the bathymetry gradient and as the bottom topography and the coastline geometry are complex in the Cape Finisterre area, we expect errors in the slope position in the model bathymetry to explain the differences observed at this station. Without any better estimate of the local bathymetry, we cannot further test this hypothesis. At Cabo Silleiro, tidal ellipse parameters are not correctly modeled. The model ellipse inclination is parallel to the isobaths which is consistent with the study of Visser et al. (1994) in well mixed conditions. Visser et al. (1994) also showed that in a region of freshwater influence, the stratification significantly influences the cross-shore component that can reach 40 % of along-shore component; this is consistent with the observed ellipse orientation. At Donostia and Matxitxako, modeled ellipses are also oriented along the slope while observed ones

Assessment of the Iberia-Biscay-Ireland configuration

C. Maraldi et al.

Title Page

Abstract

Introduction

Conclusions

References

Tables

Figures

◀

▶

◀

▶

Back

Close

Full Screen / Esc

Printer-friendly Version

Interactive Discussion



are oriented across the slope. Indeed vertical profile of observed M2 semi major axis shows a clear stratification in the surface layers which is not represented in the model (Fig. 13). Below this layer (upper 30 m) the modelled profile is in good agreement with observations for the two current profiles. As discussed in Sect. 4.3.3, the surface layers salinity suffers from an over- or under-estimation in the model with respect to observations (Fig. 15).

It should be stressed that model-data comparisons at single locations are very challenging in the sense that the modeled field can vary a lot from one grid point to the other especially in the slope area. Indeed, a small local error in the bathymetry (depth and slope) can generate large displacements of the circulation patterns. Therefore, such comparisons are not necessarily representative of the overall model performance. Here, we presented them to illustrate some physical processes at work to explain the model-data discrepancies.

4.3.2 Internal tides

We use 10 yr of TOPEX/Poseidon data combined with 7 yr of Jason-1 altimeter data spanning the period from September 1992 to January 2009 to obtain estimates of the internal tides signature in sea surface elevation. Altimetric data are not used for the validation of barotropic tides, as barotropic tides are compared to the FES2004 solution which assimilates altimetric data. The fraction of internal tides which is phase-locked with astronomical potential has sufficient coherence in both space and time for its surface signal to be detected in altimetric multi-year time series (Ray and Mitchum, 1997). We use an along-track harmonic analysis product provided by CTOH/LEGOS (Lyard, personal communication) to estimate the temporally coherent M2 component. We work with TOPEX/Poseidon/Jason1 track 137 that crosses the Armorican shelf slope at nearly right angle (Fig. 1) as we expect the M2 internal tides to propagate almost in the same direction (internal tides propagates perpendicular to the shelf break, Pairaud et al., 2010). To separate the barotropic tides from the time coherent internal tide signal, we then spatially filter the M2 real and imaginary parts so we remove the barotropic

Assessment of the Iberia-Biscay-Ireland configuration

C. Maraldi et al.

Title Page

Abstract

Introduction

Conclusions

References

Tables

Figures



Back

Close

Full Screen / Esc

Printer-friendly Version

Interactive Discussion



large scale signal (Ray and Mitchum, 1997). According to Pairaud et al. (2010) the wavelengths of baroclinic mode 1 and mode 2 are respectively 141 km and 75 km in the abyssal plain. Note that these values have been obtained using data collected during September–October 1994 and may vary with the stratification. To take into account the angle between the altimeter track and the internal tide direction of propagation we use a spatial cut-off slightly larger than the wavelength. We also filter at shorter scales to reduce the altimeter noise. Finally along track tidal components are filtered between 140 km and 210 km for mode 1 and between 60 km and 110 km for mode 2. The “residual tides” are obtained by removing the filtered signal from the harmonic components.

Figure 14 presents the along track amplitude and phase as computed from the altimetric data and from the model for mode 1 and for mode 2. It also presents the along track bathymetry. Indications attesting that the small oscillations are internal tides are: (1) oscillations are generated in the Armorican shelf slope region (45.8° N–46.0° N), (2) south of the shelf break the phase increases constantly in the Bay of Biscay which indicates that the wave propagates away from the shelf, (3) for mode 1 and mode 2 we find wavelengths of approximately $(\lambda_1, \lambda_2) = (197 \text{ km}, 76 \text{ km})$ in the altimetric data and the model; these values are slightly larger but in good agreement with theoretical values. The agreement between the altimetric and model estimates is remarkable: the misfits lie between 1 and 2 cm for the total M2 amplitude and the model shows similar wavelengths than altimetric data. Interestingly, both model and data indicate that the first mode has not the dominant surface signature in the Bay of Biscay. Minor discrepancies in the baroclinic amplitudes and phases are however observed. For mode 1 (mode 2) there is a southward (northward) shift of the model sea surface signal. For the two modes model amplitudes are slightly overestimated especially near the generation site for mode 2. As previously mentioned, errors in the model bathymetry (here for the Armorican shelf slope representation) are expected to lead to uncertainties in the tidal representation, especially close to the generation sites of internal tides.

Assessment of the Iberia-Biscay-Ireland configuration

C. Maraldi et al.

[Title Page](#)[Abstract](#)[Introduction](#)[Conclusions](#)[References](#)[Tables](#)[Figures](#)[⏪](#)[⏩](#)[◀](#)[▶](#)[Back](#)[Close](#)[Full Screen / Esc](#)[Printer-friendly Version](#)[Interactive Discussion](#)

4.3.3 Local stratification off the Basque country

The Donostia and Matxitxako deep sea buoys deployed by AZTI-Tecnalía over the slope off the Basque country provide hourly measurements of atmospheric parameters and ocean temperature and salinity from 10 m to 200 m (Rubio et al., 2012; Fig. 1, Table 4). They represent very valuable data as they are the only available time-series of temperature and salinity profiles over such a long period. The time evolutions of temperature and salinity as observed and modeled at the Matxitxako station are presented in Fig. 15. The profiles show clear seasonal stratification. The model reproduces reasonably well the rapid heating and freshening of spring 2008. The cooling and mixed-layer deepening during winter are also correctly represented. However the model underestimates the MLD-equivalent in winter (the MLD-equivalent is computed as the depth at which the density changes from the density at 10 m is 0.02). In summer 2007 we also notice that the model salinity is too low in the upper layers. This is due to the initialization from PSY2V3 which is too fresh in this region. On the contrary the model is slightly saltier in the surface layers during summer 2008. However, rapid freshening pulses during September 2008 are well represented in the model. Surface salinity uncertainties reflect mainly those on the precipitation fields; the latter are unknown but are expected to be larger in coastal areas such as northern Iberia because of orographic effects. Besides, Ferrer et al. (2009) have shown that fresh water discharge from several Spanish rivers can impact the offshore salinity conditions under specific oceano-meteorological conditions.

During winter 2007–2008, the ocean becomes warmer and saltier over the whole water column. This phenomenon is more marked in the model and affects the 350 m upper layer: it corresponds to a warm extension of the Iberian Poleward Current also called “Navidad event” (Pingree and Le Cann, 1992). This pattern is discussed later in Sect. 4.3.5.

Assessment of the Iberia-Biscay-Ireland configuration

C. Maraldi et al.

Title Page

Abstract

Introduction

Conclusions

References

Tables

Figures



Back

Close

Full Screen / Esc

Printer-friendly Version

Interactive Discussion



4.3.4 Residual currents

Data used for comparisons consist of residual currents from the surface buoys of Puer-
tos del Estado (Table 4). Figure 16 shows the observed and modelled residual currents
at Bilbao (zonal component) Estaca de Bares (zonal component) and at Cabo Silleiro
(meridional component). Both data and model time series are detided, filtered below 25
hours and one-day averaged. The results show that modelled residual currents have
some discrepancies when currents are weak, but they are relatively well reproduced
elsewhere. However the model tends to overestimate peak currents. Along the Iberian
Coast, RMS errors vary between 5.8 cm s^{-1} and 9.1 cm s^{-1} . Comparisons between
wind speed observed at buoy stations and extracted from ECMWF fields indicate that
magnitudes are significantly higher in the ECMWF fields especially during strong wind
events (not shown). Along the Iberian coast, the main current component is the along-
shore component: currents are predominantly meridional at the Cabo Silleiro station
while have a predominant zonal orientation at Estaca de Bares, Cabo Peñas, Bilbao.
This distribution of residual currents is well reproduced in the model. North of Spain,
both observations and model show clear eastward current intensifications during Jan-
uary. They are overestimated in the model and spread over a larger period. These in-
tensifications are associated with the extension of the Iberian Poleward Current along
the northern Spanish coast. In summer, some current pulses are also distinguished in
the data from mid-June to late August 2008 and are well reproduced in the model.

4.3.5 A focus on the circulation in the Southern Bay of Biscay

We now focus on the ability of the model in reproducing a typical dynamic feature of
the Southern Bay of Biscay: the warm extension of the Iberian Poleward Current along
the northern Spanish coast during winter. In this section our objective is not consis-
tency assessment; we analyse several variables or quantities that are relevant for the
Navidad occurrence (e.g. temperature and salinity anomalies in the upper layers, pole-
ward along-slope currents) and show how the model can be used as a complement

Title Page

Abstract

Introduction

Conclusions

References

Tables

Figures



Back

Close

Full Screen / Esc

Printer-friendly Version

Interactive Discussion



to available observations. The analysis of the modeled SST and sea surface salinity (SSS) in the Bay of Biscay shows a warm and salty current flowing poleward along the western and the northern Iberian Peninsula and reaching the south-western French coasts during winter 2007–2008 (Fig. 17, SSS not shown; see also wintertime salinity anomalies on Fig. 15). The extension of the Iberian Poleward Current at or near surface along the northern Iberian coasts is a recurrent feature of the fall/winter circulation of the Bay of Biscay (Frouin et al., 1990; Garcia-Soto et al., 2002; Le Cann and Serpette, 2009) and has been referred to “Navidad event” (Pingree and le Cann, 1992). The extension of the IPC and the associated warming are however very variable from one year to the other; besides it also undergoes some variability at times scales of a few day as discussed below. Its main signature is a surface warming along the coast, as it carries poleward warm water masses from the western Iberian region. Satellite observations clearly show the warm intrusion of the Iberian Poleward Current extending poleward as far as the Cantabrian shelf slope north of Spain on the 20th of January 2008 (Fig. 17). The intrusion is represented with a similar spatial extent in IBI with its leading edge reaching 3.5° W at the same date. Modeled SST is slightly warmer than observed SST within the Iberian Poleward Current and in surrounding waters; besides, the warm tongue appears to be narrower northwest of Spain. In surface, the current thermal signature is about 1°C warmer than adjacent waters in the data and in the model. It decreases poleward varying from more than 14.5°C off northwest Spain to about 13.5°C at 3° W. This corresponds to a drop of 1°C over a ~450 km distance which is in good agreement with the poleward temperature gradient obtained by Frouin et al. (1990) using satellite SST data. The current narrows from 40 km off northwest Spain to less than 30 km at 3° W. Vertical across slope sections of thermohaline fields along the warm current (not shown) indicate the core of warm and salty water flows over the upper shelf slope and extends from the surface to 350 m. The temperature field structure is illustrated with the map of 200 m temperature (Fig. 17).

Comparisons between modeled and observed along-slope residual currents (Fig. 16) indicate that the time variability of currents in the model is reasonably realistic. They

Assessment of the Iberia-Biscay-Ireland configurationC. Maraldi et al.

[Title Page](#)[Abstract](#)[Introduction](#)[Conclusions](#)[References](#)[Tables](#)[Figures](#)[⏪](#)[⏩](#)[◀](#)[▶](#)[Back](#)[Close](#)[Full Screen / Esc](#)[Printer-friendly Version](#)[Interactive Discussion](#)

also suggest that the model tends to overestimate the IPC surface currents at the Puertos del Estado buoys (e.g. Cabo Silleiro and Estaca de Bares). At Bilbao (Fig. 16) the eastward pulses in February and March are not observed; this suggests that the IPC may be penetrating too far in the Bay of Biscay in the model. The analysis of other

5 Navidad events (i.e. over other years) should be necessary to determine whether the model overestimation of the zonal extension of the IPC is a systematic bias in this configuration or if it occurred specifically for these events of February–March 2008.

The warm current transport has been estimated along the slope for sections perpendicular to the flow (see definition in the caption of Fig. 18). Considering typical temperature and salinity values along the current in the model, the transport has been computed for water masses warmer than 13.0 °C and saltier than 35.7 psu. Note that these values do not take into account the spatial gradient of temperature and salinity in the flow. The transport time evolution is shown in Fig. 18a. The warm intrusion is established in October 2007 northwest of Spain (Galicia). The flow progresses eastward along the slope around Cape Finisterre, reaches the coast off North Galicia in November and continues its intrusion in the Cantabrian Sea. North of Spain, the warm current is established until May. From the transport across each section we estimate the mean poleward flow to propagate at velocities between 13 cm s⁻¹ and 24 cm s⁻¹ which agree with typical values published (Frouin et al., 1990; Garcia-Soto et al., 2002). From

10 Fig. 18a, we also notice the warm current transport is highly variable at periods of few days and may vary from no transport to more than 2 Sv over a short period. Such variability at daily time-scales has been described by Herbert et al. (2011) during the winter 2004, from in situ observations and a numerical simulation. These authors suggest that the high-frequency variations are due to local wind forcing. When it is established, the current varies almost simultaneously at each section in response of forcing. The transport time series present a lag of 1 day between 8° W and 6° W (respectively 6° W and 3.8° W) and correlation of 0.75 (respectively 0.79) between the two transports.

Driving mechanisms of the poleward current are often attributed to the large scale meridional pressure gradient in the North Atlantic and to local wind stress (Frouin et

Assessment of the Iberia-Biscay-Ireland configuration

C. Maraldi et al.

Title Page

Abstract

Introduction

Conclusions

References

Tables

Figures

◀

▶

◀

▶

Back

Close

Full Screen / Esc

Printer-friendly Version

Interactive Discussion



al., 1990; Le Cann and Serpette, 2009). Figure 18b represents the meridional wind stress off western Iberia and of the zonal wind stress off northern Iberia, averaged over boxes defined following Le Cann and Serpette (2009). Positive values of wind stress indicate downwelling favorable conditions which are likely to force the poleward flow.

5 West of Iberia, wind stress is upwelling favorable until October 2007; then it is northward until the end of the year and is expected to provide a driving mechanism of the poleward current. When the current has reached Cape Finisterre and turns eastward, its poleward flow is maintained by eastward winds.

5 Conclusions

10 A high-resolution simulation covering the Iberia-Biscay-Ireland (IBI) region was carried out over July 2007–February 2009 within the MyOcean project (Cailleau et al., 2012). In this paper, we had three main objectives: (1) give an overview of the model configuration used for the simulation; (2) give a broad-brush account of one particular aspect of this work, namely consistency verification; this type of validation is conducted upstream
15 of the implementation of the system before it is used for production and routinely validated; it is meant to guide model development in identifying gross deficiencies in the modelling of several key physical processes; (3) show that such a regional modelling system has potential as a complement to patchy observations (an integrated approach) to give information on non-observed physical quantities and to provide links between
20 observations by identifying broader-scale patterns and processes. Objectives (2) and (3) were pursued in the year 2008.

The NEMO model was implemented with a $1/36^\circ$ horizontal resolution and 50 z-levels in the vertical. Running NEMO over coastal areas and shelf seas implied several model developments which are evolving and will still evolve depending on performance
25 requirements and user needs within MyOcean/MyOcean2. The main development concerned the free surface formulation to solve for surface gravity waves and therefore to represent the ocean response to tidal and atmospheric pressure forcing. Modelling

Assessment of the Iberia-Biscay-Ireland configuration

C. Maraldi et al.

Title Page

Abstract

Introduction

Conclusions

References

Tables

Figures



Back

Close

Full Screen / Esc

Printer-friendly Version

Interactive Discussion



Assessment of the Iberia-Biscay-Ireland configurationC. Maraldi et al.

[Title Page](#)[Abstract](#)[Introduction](#)[Conclusions](#)[References](#)[Tables](#)[Figures](#)[Back](#)[Close](#)[Full Screen / Esc](#)[Printer-friendly Version](#)[Interactive Discussion](#)

tides implied as well to revisit the open-boundary conditions formulation. Large efforts were also pursued on the vertical mixing: we included the parameterization of Craig and Banner (1994) to account for the surface wave-induced turbulence and revisited the bottom stress parameterization as well as the bottom roughness values impact over the shelf circulation. We also worked on the solar radiation penetration to better account for the different optical properties between waters over the shelf and in the deep ocean, and improved river runoff forcing by prescribing flow rates from 33 rivers. The configuration became operational in early 2012.

We then examined domain-wide consistency verification results in terms of barotropic tides, transports, sea surface temperature and stratification. We also focused with more detail on two dynamical sub-regions: the Celtic shelves and the Bay of Biscay slope and deep regions; there, the model-data consistency was checked, not exhaustively, but for a few important variables and processes such as tidal currents, tidal fronts, internal tides, residual elevation. Although a number of relatively minor points have been raised in the paper, or points not in the IBI system specifications (e.g., details of the MW outflow), no major discrepancy with respect to expectations was identified. However the study highlighted a few grey areas requiring more specific attention and testing, as well as priorities for improvement.

For instance, the analysis of the tidal elevations and current fields suggests that local improvements in the bathymetry are essential to better represent the tidal propagation, the bottom mixing as well as the generation of internal tides. Such improvements are also essential in regions of downscaling to finer-grid models, as well as to facilitate point-comparisons with observations, a small error in the bathymetry (depth and slope) being able to generate large displacements of the circulation patterns.

Another important forcing in coastal areas is freshwater discharge, mainly from rivers. The analysis of the baroclinic tidal surface signal points out at at least two regions in the Bay of Biscay where the surface stratification in the model was probably poorly represented (however, the lack of available subsurface hydrological data will not permit direct comparisons). In these regions and according to past studies (e.g. Ferrer

et al., 2009), runoffs from the Galician and the Basque rías have a significant impact on the local stratification but are not taken into account in our model configuration. Tests are necessary to quantify the impact of local changes of the surface stratification at different time-scales on the baroclinic tidal currents. More generally, it becomes evident
5 that a large effort for a more realistic representation of continental water discharge including the runoffs from small rivers is needed at least in these areas. Following some of our consistency checks, daily runoffs (instead of monthly climatological ones) are now prescribed in the operational version of this IBI configuration.

Other points follow. Further increases in horizontal and vertical resolution would allow
10 to better serving some types of applications, such as biological connectivity and surface currents, the latter being probably strongly influenced by wave-current interactions (Law-Chune et al., 2012). Further tuning of the bottom friction and its spatial dependence on the seabed type may improve the solution locally for tides and surges, with impacts on SST distribution in frontal regions. Uncertainties in atmospheric forcings are
15 likely to drive model errors on surface circulation and on tracer distributions via wind-driven turbulence. Errors are expected to occur on high-frequencies and small-scale patterns, especially close to the coasts where the effects of small-scale orography are poorly represented. Stochastic modelling would provide an interesting framework for the assessment of atmospheric uncertainties impacts (e.g. Quattrochi et al., 2012). We
20 also suggest that R&D studies should be carried out to accompany the development of atmospheric downscaling for operational systems.

The model-data comparisons presented in this paper did not include an error analysis; for this, we need reliable estimates of uncertainties on the data, which are generally unavailable. Such estimates are required for instance in order to better identify the
25 source of the discrepancies between the simulations and the gridded HF radar data in the vicinity of the Ushant front. The representativeness of local measurements (such as *T/S* profiles from the EN3 data base or current time-series from the Puertos del Estado buoy network) is a general problem, linked to the problem of upscaling local information when comparing to increasingly high-resolution simulations. We also suggest to

Assessment of the Iberia-Biscay-Ireland configurationC. Maraldi et al.

[Title Page](#)[Abstract](#)[Introduction](#)[Conclusions](#)[References](#)[Tables](#)[Figures](#)[Back](#)[Close](#)[Full Screen / Esc](#)[Printer-friendly Version](#)[Interactive Discussion](#)

complement the datasets used for the consistency checks: for example, both Ferrybox T/S data and satellite altimetry data would be a nice complement, both datasets being characterized by repetitive sampling.

In the last section of this paper, we investigated the representation of the winter slope current along the northern Spanish coast (Navidad event). As very few data were available, this test is an illustration of the potential of our modelling system as a complement to observations within an integrated approach. We examined diagnostics on observed (e.g. surface currents) and non-observed (e.g. along-slope transport) quantities, that could serve as a basis to define indices and that provide links between observations.

Lastly, the relatively high (2–3 km) horizontal resolution used clearly pushes the model into the sub-mesoscale permitting regime over much of the domain and allows a significant part of the internal wave spectrum to be resolved. This seems to be the natural way forward to anticipate future high resolution satellite observing systems such as SWOT (Surface Water and Ocean Topography).

Acknowledgements. The research leading to these results have received funding from the European Community's Seventh Framework Programme FP7/2007-2013 under grant agreement no. 218812 (MyOcean) and through its partnership with CNRS (Centre National de la Recherche Scientifique).

The regional bathymetries used for the study have been provided by Ifremer, the French Navy Hydrographic and Oceanographic Service (Service Hydrographique et Océanographique de la Marine, SHOM) and the North West Shelf Operational Oceanographic System. Tide gauge data used were provided by Puertos del Estado, the Marine Institute, the Danish Meteorological Institute and tide gauge data from SHOM, from the British Oceanographic Data Center and from GLOSS were provided by Collecte Localisation Satellites (CLS) via the Badommar specific database are also used. The MODIS SST image was obtained through the online JPL PO.DAAC Ocean ESIP Tool (POET) at the Physical Oceanography Distributed Active Archive Center (PO.DAAC), NASA Jet Propulsion Laboratory, Pasadena, CA (<http://podaac.jpl.nasa.gov/poet>).

The authors gratefully acknowledge the receipt of buoy data from Puertos del Estado, Météo France, the Marine Institute and the AZTI, of along track altimetric data from LEGOS/CTOH,

Assessment of the Iberia-Biscay-Ireland configuration

C. Maraldi et al.

Title Page

Abstract

Introduction

Conclusions

References

Tables

Figures

◀

▶

◀

▶

Back

Close

Full Screen / Esc

Printer-friendly Version

Interactive Discussion



of historical current meter data from BODC and of radar HF data provided by Fabrice Arduin and SHOM. Outflow estimates at the Gibraltar Strait have been obtained through the monitoring station at Espartel sill, west Gibraltar, which is deployed and serviced within the frame of the Spanish-funded projects INGRES (REN2003-01608, CTM2006-02326, CTM2009-05810E and CTM2010-21229). We acknowledge J. Garcia Lafuente, PI of these projects, for providing us with this information. We thank the Mercator Ocean teams, Charly Reignier and Clément Bricaud whose hard work made this study possible. This study also benefited from fruitful discussions with Gildas Cambon concerning the Ushant thermal front.



The publication of this article is financed by CNRS-INSU.

References

- Adcroft, A. and Campin, J.-M.: Rescaled height coordinates for accurate representation of free-surface flows in ocean circulation models, *Ocean Model.*, 7, 269–284, 2004.
- Alvarez, M., Perez, F. F., Bryden, H. L., and Rios, A. F.: Physical and biochemical transports structure in the North Atlantic subpolar gyre, *J. Geophys. Res.*, 109, C03027, doi:10.1029/2003JC002015, 2004.
- Arbic, B. K., Wallcraft, A. J., and Metzger, E. J.: Concurrent simulation of the eddy general circulation and tides in a global ocean model, *Ocean Model.*, 32, 175–187, 2010.
- Barnier, B., Madec, G., Penduff, T., Molines, J.-M., Treguier, A.-M., Le Sommer, J., Beckmann, A., Biastoch, A., Böning, C., Dengg, J., Derval, C., Durand, E., Gulev, S., Remy, E., Talandier, C., Theetten, S., Maltrud, M., McClean, J., and De Cuevas, B.: Impact of partial steps and momentum advection schemes in a global ocean circulation model at eddy-permitting resolution, *Ocean Dynam.*, 56, 543–567, doi:10.1007/s10236-006-0082-1, 2006.

Assessment of the Iberia-Biscay-Ireland configuration

C. Maraldi et al.

Title Page

Abstract

Introduction

Conclusions

References

Tables

Figures



Back

Close

Full Screen / Esc

Printer-friendly Version

Interactive Discussion



Assessment of the Iberia-Biscay-Ireland configuration

C. Maraldi et al.

Title Page

Abstract

Introduction

Conclusions

References

Tables

Figures

◀

▶

◀

▶

Back

Close

Full Screen / Esc

Printer-friendly Version

Interactive Discussion



- Becker, J. J., Sandwell, D. T., Smith, W. H. F., Braud, J., B. Binder, B., Depner, J., Fabre, D., Factor, J., Ingalls, S., Kim, S.-H., Ladner, R., Marks, K., Nelson, S., Pharaoh, A., Trimmer, R., Von Rosenberg, J., Wallace, G., and Weatherall, P.: Global bathymetry and elevation data at 30 arc seconds resolution: SRTM30 PLUS, *Mar. Geod.*, 32, 355–371, 2009.
- 5 Benzhora, M. and Millot, C.: Characteristics and circulation of the surface and intermediate water masses off Algeria, *Deep-Sea Res.*, 42, 1803–1830, 1995.
- Bernie, D. J., Woolnough, S. J., Slingo, J. M., and Guilyardi, E.: Modelling diurnal and intraseasonal variability of the ocean mixed layer, *J. Climate*, 18, 1190–1202, 2005.
- Blayo, E. and Debreu, L.: Revisiting open boundary conditions, from the point of view characteristic variables, *Ocean Model.*, 9, 231–253, 2005.
- 10 Brown, J. and Gmitrowitz, E. M.: Observations of the transverse structure and dynamics of the low frequency flow through the North Channel of the Irish Sea, *Cont. Shelf Res.*, 15, 1133–1156, 1995.
- Brown, J., Carrillo, L., Fernanda, L., Horsburgh, K. J., Hill, A. E., Young, E. F., and Medler, K. J.: Observations of the physical structure and seasonal jet-like circulation of the Celtic Sea and St. George's Channel of the Irish Sea, *Cont. Shelf Res.*, 23, 533–561, 2003.
- Burchard, H., Deleersnijder, E. and Stoyan, G.: Some numerical aspects of turbulence-closure models, in *Marine Turbulence: Theories, Observations, and Models. Results of the CARTUM Project*, Cambridge University Press, 2005.
- 20 Cailleau, S., Chanut, J., Lellouche, J.-M., Levier, B., Maraldi, C., Refray, G., and Sotillo, M. G.: Towards a regional ocean forecasting system for the IBI (Iberia-Biscay-Ireland area): developments and improvements within the ECOOP project framework, *Ocean Sci.*, 8, 143–159, doi:10.5194/os-8-143-2012, 2012.
- Candela, J.: The Gibraltar Strait and its role in the dynamics of the Mediterranean Sea, *Dynam. Atmos. Oceans*, 15, 3–5, 267–300, 1991.
- 25 Canuto, V. M., Howard, A. M., Cheng, Y., and Dubovikov, M. S.: Ocean turbulence. Part I: one-point closure model momentum and heat vertical diffusivities, *J. Phys. Oceanogr.*, 31, 1413–1426, 2001.
- Carrère, L. and Lyard, F.: Modelling the barotropic response of the global ocean to atmospheric wind and pressure forcing – comparisons with observations, *Geophys. Res. Lett.*, 30, 1275, doi:10.1029/2002GL016473, 2003.
- 30

Assessment of the Iberia-Biscay-Ireland configuration

C. Maraldi et al.

Title Page

Abstract

Introduction

Conclusions

References

Tables

Figures

◀

▶

◀

▶

Back

Close

Full Screen / Esc

Printer-friendly Version

Interactive Discussion



- Charria, G., Lazure, P., Le Cann, B., Serpette, A., Reverdin G., Louazel, S., Batifoulier, F., Dumas, F., Pichon, A., and Morel, Y.: Surface layer circulation derived from Lagrangian drifters in the Bay of Biscay, *J. Mar. Syst.*, doi:10.1016/j.jmarsys.2011.09.015, in press, 2011.
- Craig, P. D. and Banner, M. L.: Modeling wave-enhanced turbulence in the ocean surface layer, *J. Phys. Oceanogr.*, 24, 2546–2559, 1994.
- Coelho, H. S., Neves, R. J. J., White, M., Leitao, P. C., and Santos, A. J.: A model for ocean circulation on the Iberian coast, *J. Mar. Syst.*, 32, 153–179, 2002.
- Davies, A. M. and Aldridge, J. N.: A numerical model study of parameters influencing tidal currents in the Irish Sea, *J. Geophys. Res.*, 98, 7049–7067, 1993.
- Davies, A. M., Kwong, S. C. M., and Flather, R. A.: A three-dimensional model of diurnal and semidiurnal tides on the European shelf, *J. Geophys. Res.*, 102, 8625–8656, 1997.
- Drévilion, M., Bourdallé-Badie, R., Derval, C., Drillet, Y., Lellouche, J.-M., Rémy, E., Tranchant, B., Benkiran, M., Greiner, E., Guinehut, S., Verbrugge, N., Garric, G., Testut, C.-E., Laborie, M., Nouel, L., Bahurel, P., Bricaud, C., Crosnier, L., Dombrowsky, E., Durand, E., Ferry, N., Hernandez, F., Galloudec, O., Messal, F., and Parent, L.: The GODAE Mercator-Océan global ocean forecasting system: results, applications and prospects, *J. Oper. Oceanogr.*, 1, 51–57, 2008.
- Dombrowsky, E., Bertino, L., Brassington, G. B., Chassignet, E. P., Davidson, F., Hurlburt, H. E., Kamachi, M., Lee, T., Martin, M. J., Mei, S., and Tonani, M.: GODAE systems in operation, *Oceanography*, 22, 80–95, 2009.
- Egbert, G., Bennett, A., and Foreman, M.: TOPEX/Poseidon tides estimated using a global inverse model, *J. Geophys. Res.*, 99, 24821–24852, 1994.
- Ellett, D. J. and Martin, J. H. A.: The physical and chemical oceanography of the Rockall Channel, *Deep-Sea Res.*, 20, 585–625, 1973.
- Fanjul, E. A., Gomez, B. P., and Rodriguez, I.: A description of the tides in the Eastern North Atlantic, *Prog. Oceanogr.*, 40, 217–244, 1997.
- Ferrer, L., Fontán, A., Mader, J., Chust G., González, M., Valencia, V., Uriarte, A., and Collins, M. B.: Low-salinity plumes in the oceanic region of the Basque Country, *Cont. Shelf Res.*, 29, 970–984, doi:10.1016/j.csr.2008.12.014, 2009.
- Flather, R. A.: A tidal model of the North-East Pacific, *Atmos. Ocean*, 25, 22–45, 1987.
- Foreman, F. G. G.: Manual for tidal heights analysis and predictions, Institute of Ocean Sciences, Patricia Bay, *Pacif. Mar. Rep.*, 77, 101 pp., 1977.

Assessment of the Iberia-Biscay-Ireland configuration

C. Maraldi et al.

Title Page

Abstract

Introduction

Conclusions

References

Tables

Figures

◀

▶

◀

▶

Back

Close

Full Screen / Esc

Printer-friendly Version

Interactive Discussion



Frail-Nuez, E., Plaza, F., Hernandez-Guerra, A., Vargas-Yanez, M., and Lavin, A.: Mass transport in the Bay of Biscay from an inverse box model, *J. Geophys. Res.*, 113, C06023, doi:10.1029/2007JC004490, 2008.

5 Frouin, R., Fiúza, A. F. G., Ambar, I., and Boyd, T.: Observations of poleward surface current off the coasts of Portugal and Spain during winter, *J. Geophys. Res.*, 95, 679–691, 1990.

García-Lafuente, J., Díaz del Río, G., and Sánchez Berrocal, C.: Vertical and bottom intensification of tidal currents off Northwestern Spain, *J. Mar. Syst.*, 62, 55–70, 2006.

10 Garcia-Soto, C., Pingree, R. D., and Valdés, L.: Navidad development in the Southern Bay of Biscay: climate change and swoddy structure from remote sensing and in situ measurements, *J. Geophys. Res.*, 107, doi:10.1029/2001JC001012, 2002.

Gohin, F., Loyer, S., Lunven, M., Labry, C., Froidefond, J. M., Delmas, D., Huret, M., and Herbland, A.: Satellite-derived parameters for biological modelling in coastal waters: illustration over the eastern continental shelf of the Bay of Biscay, *Remote Sens. Environ.*, 112, 3329–3340, 2005.

15 Herbert, G., Ayoub, N., Marsaleix, P., and Lyard, F.: Signature of the coastal circulation variability in altimetric data in the Southern Bay of Biscay during winter and fall 2004, *J. Mar. Syst.*, 88, 139–158, 2011.

Holliday, N. P., Pollard, R. T., Read, J. F., and Leach, H.: Water mass properties and fluxes in the Rockall Trough, 1975–1998, *Deep-Sea Res Pt. I*, 47, 1303–1332, 2000.

20 Holt, J. T. and James, I. D.: An *s* coordinate density evolving model of the Northwest European continental shelf – 1, Model description and density structure, *J. Geophys. Res.*, 106, 14015–14034, 2001.

Holt, J. and Umlauf, L.: Modelling the tidal mixing fronts and seasonal stratification on the Northwest European shelf, *Cont. Shelf Res.*, 28, 887–903, 2008.

25 Holt, J. T., James, I. D., and Jones, J. E.: An *s* coordinate density evolving model of the Northwest European continental shelf – 2, seasonal currents and tides, *J. Geophys. Res.*, 106, 14035–14053, 2001.

Holt, J. T., Allen, J. I., Proctor, R., and Gilbert, F.: Error quantification of a high-resolution coupled hydrodynamic-ecosystem coastal-ocean model: Part 1 model overview and assessment of the hydrodynamics, *J. Mar. Syst.*, 57, 167–188, 2005.

30 Howarth, M. J.: Non-tidal flow in the North Channel of the Irish Sea. *Hydrodynamics of Semi-Enclosed Seas: Proceedings of the 13th International Liege Colloquium on Ocean Hydrodynamics*, edited by: Nihoul, J. C. J., Elsevier, 205–241, 1982.

Assessment of the Iberia-Biscay-Ireland configuration

C. Maraldi et al.

Title Page

Abstract

Introduction

Conclusions

References

Tables

Figures

◀

▶

◀

▶

Back

Close

Full Screen / Esc

Printer-friendly Version

Interactive Discussion



- Howe, M. R.: Current and hydrological measurements in the Mediterranean Undercurrent near Cape St. Vincent, *Oceanol. Acta*, 7, 163–168, 1984.
- Ingleby, B. and Huddleston, M.: Quality control of ocean temperature and salinity profiles historical and real time data, *J. Mar. Syst.*, 65, 158–175, 2007.
- 5 Jorge da Silva, A.: The slope current off the West Iberian coast in autumn, *ICES C.M.* 1996/S:35, 1996.
- Kaplan, D. M. and Lekien F.: Spatial interpolation and filtering of surface current data based on open-boundary modal analysis, *J. Geophys. Res.*, 112, C12007, doi:10.1029/2006JC003984, 2007.
- 10 Large, W. G. and Yeager S. G.: Diurnal to decadal global forcing for ocean and sea-ice models: the data sets and flux climatologies. NCAR Technical Note: NCAR/TN-460+STR. CGD Division of the National Center for Atmospheric Research, 2004.
- Le Borgne, P., Marsouin, A., Orain, F., and Roquet, H.: Operational sea surface temperature bias adjustment using AATSR data, *Remote Sens. Environ.*, 116, 93–106, 2011.
- 15 Le Boyer, A., Cambon, G., Danialt, N., Herbette, S., Le Cann, B., Marié, L., and Morin, P.: Observations of the Ushant tidal front in September 2007, *Cont. Shelf Res.*, 29, 1026–1037, 2009.
- Le Cann, B. and Serpette, A.: Intense warm and saline upper ocean inflow in the Southern Bay of Biscay in autumn-winter 2006–2007, *Cont. Shelf Res.*, 29, 1014–1025, 2009.
- 20 Lellouche, J.-M., Le Galloudec, O., Drévilion, M., Régnier, C., Desportes, C., Tranchant, B., Testut, C.-E., Greiner, E., Garric, G., Bourdallé-Badie, R., Bricaud, C., Ferry, N., Drillet, Y., Daudin, A., and De Nicola, C.: Overview and scientific assessment of the MyOcean/Mercator Océan global ocean monitoring and forecasting system, *Ocean Sci. Discuss.*, in preparation, 2012.
- 25 Leonard, B. P.: A stable and accurate convective modelling procedure based on quadratic upstream interpolation, *Comput. Methods Appl. Mech. Eng.*, 19, 59–98, 1979.
- Le Traon P. Y., and Gauzelin P. : Response of the Mediterranean mean sea level to atmospheric pressure forcing. *J. Geophys. Res.-oceans*, 102, 973–984, 1997.
- Lherminier, P., Mercier, H., Gourcuff, C., Alvarez, M., Bacon, S., and Kermabon, C.: Transports across the 2002 Greenland–Portugal Ovide section and comparison with 1997, *J. Geophys. Res.*, 112, C07003, doi:10.1029/2006JC003716, 2007.
- 30 Lyard, F., Lefevre, F., Letellier, T., and Francis, O.: Modelling the global ocean tides: modern insights from FES2004, *Ocean Dynam.*, 56, 394–415, 2006.

Assessment of the Iberia-Biscay-Ireland configuration

C. Maraldi et al.

Title Page

Abstract

Introduction

Conclusions

References

Tables

Figures

◀

▶

◀

▶

Back

Close

Full Screen / Esc

Printer-friendly Version

Interactive Discussion



- Madec, G.: NEMO Ocean General Circulation Model Reference Manuel, Internal Report, LODYC/IPSL, Paris, 2008.
- Madec, G., Delecluse, P., Imbard, M., and Lévy, C.: OPA 8.1 Ocean general circulation model reference manual, Notes du Pôle de Modélisation no 11, Institut Pierre-Simon Laplace, Paris, France, 91p, 1998.
- 5 Mariette, V. and Le Cann, B.: Simulation of the formation of Ushant thermal front, Cont. Shelf Res., 4, 637–660, 1985.
- Mauritzen, C., Morel, Y., and Paillet, J.: On the influence of Mediterranean water on the central waters of the North Atlantic Ocean, Deep-Sea Res. Pt. I, 48, 347–381, 2001.
- 10 Mazé, J. P., Arhan, M., and Mercier, H.: Volume budget of the eastern boundary layer off the Iberian Peninsula, Deep-Sea Res. Pt. I, 44, 1543–1574, 1997.
- Morel, A., Huot, Y., Gentili, B., Werdell, P. J., Hooker, S. B., and Franz, B. A.: Examining the consistency of products derived from various ocean color sensors in open ocean (Case 1) waters in the perspective of a multi-sensor approach, Remote Sens. Environ., 111, 69–88, 2007.
- 15 Muller, H., Blanke, B., Dumas, F., Lekien, F., and Mariette, V.: Estimating the Lagrangian residual circulation in the Iroise Sea, J. Mar. Syst., 78, S17–S36, 2009.
- O’Dea, E. J., Arnold, A. K., Edwards, K. P., Furner, R., Hyder, P., Martin, M. J., Siddorn, J. R., Storkey, D., While, J., Holt, J. T., and Liu, H.: An operational ocean forecast system incorporating NEMO and SST data assimilation for the tidally driven European North-West shelf, J. Oper. Ocean., 5, 3–17, 2012.
- 20 Otto, L., Zimmerman, J. T. F., Furnes, G. K., Mork, M., Saetre, R., and Becker, G.: Review of the physical oceanography of the North Sea, Netherlands, J. Sea Res., 26, 161–238, 1990.
- Pairaud, I., Auclair, F., Marsaleix, P., Lyard, F., and Pichon, A.: Dynamics of the semi-diurnal and quarter-diurnal tides in the Bay of Biscay. Part 2: Baroclinic tides, Cont. Shelf Res., 30, 253–269, 2010.
- 25 Peliz, A., Dubert, J., Marchesiello, P., and Tele-Macado, A.: Surface circulation in the Gulf of Cadiz: model and mean flow structure, J. Geophys. Res., 112, C11015, doi:10.1029/2007JC004159, 2007.
- 30 Peliz, A., Marchesiello, P., Santos, A. M. P., Dubert, J., Tele-Macado, A., Marta-Almeida, M., and Le Cann, B.: Surface circulation in the Gulf of Cadiz: 2. Inflow-Outflow coupling and the Gulf of Cadiz slope current, J. Geophys. Res., 114, C03011, doi:10.1029/2008JC004771, 2009.

Assessment of the Iberia-Biscay-Ireland configuration

C. Maraldi et al.

Title Page

Abstract

Introduction

Conclusions

References

Tables

Figures

◀

▶

◀

▶

Back

Close

Full Screen / Esc

Printer-friendly Version

Interactive Discussion



- Pérez, B., Brouwer, R., Beckers, J., Paradis, D., Balseiro, C., Lyons, K., Cure, M., Sotillo, M. G., Hackett, B., Verlaan, M., and Fanjul, E. A.: ENSURF: multi-model sea level forecast – implementation and validation results for the IBIROOS and Western Mediterranean regions, *Ocean Sci.*, 8, 211–226, doi:10.5194/os-8-211-2012, 2012.
- 5 Pichon, A. and Correard, S.: Internal tides modelling in the Bay of Biscay. Comparisons with observations, *Sci. Mar.*, 70, 65–88, 2006.
- Pimentel, S., Haines, K., and Nichols, N. K.: Modeling the diurnal variability of sea surface temperatures, *J. Geophys. Res.*, 113, C11004, doi:10.1029/2007JC004607, 2008.
- Pingree, R. D. and Le Cann, B.: Structure, strength and seasonality of the slope
10 currents in the Bay of Biscay region, *J. Mar. Biol. Assoc. UK*, 70, 857–885, doi:10.1017/S0025315400059117, 1990.
- Pingree, R. D. and Le Cann, B.: Three anticyclonic SlopeWater oceanic eDDIES (SWODDIES) in the Southern Bay of Biscay in 1990, *Deep-Sea Res.*, 39, 1147–1175, 1992.
- Pingree, R. D., Mardell, G. T., and New, A. L.: Propagation of internal tides from the upper
15 slopes of the Bay of Biscay, *Nature*, 321, 154–158, 1986.
- Pinot, J.-M., Lopez-Jurado, J. L., and Riera, M.: The CANALES experiment (1990–1998). Inter-annual, seasonal, and mesoscale variability of the circulation in the Balearic Channels, *Prog. Oceanogr.*, 55, 335–370, 2002.
- Prandle, D., Ballard, G., Flatt, D., Harrison, A. J., Jones, S. E., Knight, P. J., Loch, S., Mc-
20 Manus, J., Player, R., and Tappin, A.: Combining modelling and monitoring to determine fluxes of water, dissolved and particulate metals through the Dover Strait, *Cont. Shelf Res.*, 16, 237–257, 1996.
- Rasclé, N., F. Arduin, P. Queffelec, and D. Croizé-Fillon: A global wave parameter database for geophysical applications. Part 1: Wave-current-turbulence interaction parameters for the open ocean based on traditional parameterizations, *Ocean Model.*, 25, 154–171, 2008.
- 25 Ray, R. D. and Mitchum, G. T.: Surface manifestation of internal tides in the deep ocean: observation from altimetry and island gauges, *Prog. Oceanogr.*, 40, 135–162, 1997.
- Rhein, M. and Hinrichsen, H. H.: Modification of Mediterranean water in the Gulf of Cadiz, studied with hydrographic, nutrient and chlorofluoromethane data, *Deep-Sea Res. Pt. I*, 40, 267–291, 2003.
- 30 Roullet, G. and Madec, G.: Salt conservation, free surface, and varying levels: A new formulation for ocean general circulation models, *J. Geophys. Res.*, 105, 23927–23942, 2000.

- Rubio, A., Fontán, A., Lazure, P., González, M., Valencia, V., Ferrer, L., Mader, J., and Hernández, C.: On the seasonal variability of currents and temperature in waters of the continental slope, Southern Bay of Biscay, *J. Mar. Syst.*, submitted, 2012.
- 5 Sánchez Román, A., Sannino, G., García Lafuente, J., Carillo, A., and Criado Aldeanueva, F.: Transport estimates at the western section of the Strait of Gibraltar: a combined experimental and numerical modelling study, *J. Geophys. Res.*, 114, C06002, doi:10.1029/2008JC005023, 2009.
- 10 Shchepetkin, A. F. and McWilliams, J. C.: The regional ocean modelling system (ROMS): a split-explicit, free-surface, topography-following-coordinate oceanic model, *Ocean Model.*, 9, 347–404, 2004.
- SHOM: Courants de marée de la côte Ouest de Bretagne, de Goulven à Penmarch, SHOM Publication 560, 1994.
- Simpson, J. H. and Hunter, J. R.: Fronts in the Irish Sea, *Nature*, 250, 404–406, 1974.
- 15 Sotillo, M. G., Jordi, A., Ferre M. I., Conde, J., Tintoré, J., and Alvarez-Fanjul, E.: The ESEOO Regional Ocean Forecasting System, Proceedings of the Seventeenth International Offshore and Polar Engineering Conference, Lisbon, Portugal, July 1–6, 2007.
- Tsimplis, M. N. and Bryden, H. L.: Estimation of the transports through the Strait of Gibraltar, *Deep-Sea Res. Pt. I*, 47, 2219–2242, 2000.
- 20 Umlauf, L. and Burchard, H.: A generic length-scale equation for geophysical turbulence models, *J. Mar. Res.*, 61, 235–265, 2002.
- Visser, A. W., Souza, A. J., Hessner, K., and Simpson, J. H.: The effect of stratification on tidal current profiles in a region of freshwater influence, *Oceanol. Acta*, 17, 369–382, 1994.
- Warner, J. C., Sherwood, C. R., Arango, H. G., and Signell, R. P.: Performance of four turbulence closure methods implemented using a generic length scale method, *Ocean Model.*, 8, 81–113, 2005.
- 25 White, M. and Bowyer, P.: The shelf-edge current north-west of Ireland, *Ann. Geophys.*, 15, 1076–1083, doi:10.1007/s00585-997-1076-0, 1997.

Assessment of the Iberia-Biscay-Ireland configuration

C. Maraldi et al.

[Title Page](#)
[Abstract](#)
[Introduction](#)
[Conclusions](#)
[References](#)
[Tables](#)
[Figures](#)
[Back](#)
[Close](#)
[Full Screen / Esc](#)
[Printer-friendly Version](#)
[Interactive Discussion](#)


Assessment of the Iberia-Biscay-Ireland configuration

C. Maraldi et al.

Title Page

Abstract

Introduction

Conclusions

References

Tables

Figures

◀

▶

◀

▶

Back

Close

Full Screen / Esc

Printer-friendly Version

Interactive Discussion



Table 1. RMS error of the complex amplitude difference between observed and modelled tidal components. Units are in cm. The studies of Holt et al. (2001, 2005) cover the 48° N/63° N/12° W/13° E region and the 48° N/62° N/12° W/13° E region respectively and results obtained in the studies of Holt et al. (2001, 2005) are presented for comparisons (values in brackets). The Gulf of Cadiz and West Iberian region is delimited by 36.5° N/44° N/10.5° W/6.5° W; the Bay of Biscay region is delimited by 43° N/48.5° W/8° W/1° W; the Irish Sea is delimited by 51° N/56° N/9° W/3° W; the English Channel is delimited by 48.5° N/51.5° N/5° W/2° E; the North Sea region is delimited by 51.5° N/60° N/4.5° W/7.5; and the Baltic region is delimited by 56° N/59° N/7.5° W/13° W.

Regional	M2	S2	K1	O1	M4
Global	21.6	8.0	1.8	1.3	7.1
Gulf of Cadiz and West Iberian Plateau	3.2	3.4	0.9	0.4	0.6
Bay of Biscay	29.5	10.6	1.2	0.8	0.8
Irish Sea	25.9	10.1	1.7	1.3	11.1
English Channel	23.6	8.1	1.5	1.9	7.5
North Sea	14.7	4.7	2.7	1.0	6.2
Baltic	29.8	9.0	2.4	2.1	0.9
Holt et al. (2001)	24.1 (21.6)	8.8 (12.0)	2.1 (5.5)	1.5 (3.1)	8.3 (6.8)
Holt et al. (2005). Amplitudes only	12.6 (16.3)	4.2 (7.3)	1.7 (2.4)	1.0 (2.6)	7.0 (5.0)

Assessment of the Iberia-Biscay-Ireland configuration

C. Maraldi et al.

Table 2. RMS between observed and modelled (runbc) tidal ellipse parameters. Units are in cm s^{-1} . Statistics are also performed over the area covered by the studies of Holt et al. (2001, 2005) ($48^\circ \text{N}/62^\circ \text{N}/12^\circ \text{W}/13^\circ \text{E}$) and results obtained in the studies of Holt et al. (2001, 2005) are presented for comparisons (values in brackets). The West Iberian Plateau region is delimited by $37^\circ \text{N}/44^\circ \text{N}/10.5^\circ \text{W}/8.5^\circ \text{W}$; the Bay of Biscay is delimited by $43^\circ \text{N}/56^\circ \text{W}/10^\circ \text{W}/1^\circ \text{W}$; the Irish Sea is delimited by $51^\circ \text{N}/56^\circ \text{N}/9^\circ \text{W}/3^\circ \text{W}$ and the North Sea region is delimited by $51.5^\circ \text{N}/60^\circ \text{N}/4.5^\circ \text{W}/7.5^\circ \text{E}$.

	SEMA	SEMI	Inc	Pha
Barotropic ellipses (M_2)				
IBI domain	4.8	3.9	23.8	27.0
West Iberian Plateau	4.2	0.4	31.6	22.6
Bay of Biscay	4.1	6.9	33.7	45.5
Irish Sea	5.3	3.0	3.0	3.9
North Sea	3.3	2.3	9.5	9.0
Holt et al. (2001, 2005)	3.5	2.0	9.2	12.0
	(11.4, 5.8)	(–, –)	(13.1, –)	(–, –)
Baroclinic ellipses (buoys, M_2)				
IBI domain	4.4	2.6	22.1	31.3
Baroclinic ellipses (radar, M_2)				
Iroise sea (depth >50 m)	4.6	2.5	5.1	5.6
Baroclinic ellipses (radar, M_4)				
Iroise sea (depth >50 m)	1.1	0.3	17.1	39.6

[Title Page](#)
[Abstract](#)
[Introduction](#)
[Conclusions](#)
[References](#)
[Tables](#)
[Figures](#)
[Back](#)
[Close](#)
[Full Screen / Esc](#)
[Printer-friendly Version](#)
[Interactive Discussion](#)


Assessment of the Iberia-Biscay-Ireland configuration

C. Maraldi et al.

Table 3. Transport estimates from the model and the literature. Model transports are estimated from monthly fields and mean and standard deviation values are presented. Units are Sv. Values in green (resp. in red) indicate net northward transports (resp. net southward transports) for meridional sections or net eastward transports (net westward transports) for zonal sections as computed from observations. Values in black indicate net transports. Transport classes are defined using temperature classes (T), salinity classes (S) density classes (σ), depth classes (z) or with no classes (NO).

Section name	Section number	Ext. 1	Ext. 2	Transport classes	Model values Mean/StdDev	Published Estimations	References
Azores Current	1	−14.00E 33.00N	−14.00E 37.00N	$z < 1500$	15.10/4.53 −12.25/6.17	13.7 −4.7	Peliz et al. (2007)
Gibraltar	2	−5.74E 35.70N	−5.74E 36.20N	$S < 37.25$ $S > 37.25$	0.48/0.05 −0.49/0.05	0.66−0.97 −0.84−−0.57	Tsimpis and Bryden (2000); Lafuente et al. (2002)
Cadiz Gulf	3	−8.50E 32.00N	−8.50E 38.20N	$\sigma_j < 31.7$ $31.7 < \sigma_j$	1.77/0.24 −0.04/0.16	3.1 −2.8	Mauritzen et al. (2001)
North Cadiz Gulf	4	−8.50E 35.40N	−8.50E 38.20N	$32.0 < \sigma_j < 36.8$	−0.74/1.07	−6.5−−2.7	Howe (1984); Rhein and Hinrichsen (1993); Mauritzen et al. (2001)
South Portugal	5	−8.70E 37.60N	−11.00E 37.60N	$\sigma < 27.25$ $27.25 < \sigma < 32.35$	0.15/0.42 3.02/2.73	2.7−5.7 1.2−5.2	Jorge da Silva (1996); Mazé et al. (1997); Coelho et al. (2002)
Portugal	6	−20.00E 40.10N	−8.10E 40.00N	$\sigma < 27.7$ $27.7 < \sigma < 36.98$ $36.98 < \sigma < 45.85$ $45.85 < \sigma$	−1.07/0.61 −1.35/3.17 0.27/1.32 0.68/0.54	0.5−2.8 −1.4−0.5 −1.3−0.5 0.8−1.6	Alvarez et al. (2004); Lherminier et al. (2007)
Galicia	7	−9.10E 43.00N	−10.50E 43.00N	$\sigma < 27.25$ $27.25 < \sigma < 32.35$ $z < 400$ $400 < z < 900$ $900 < z < 1500$	0.32/0.33 3.63/1.66 1.71/1.11 1.72/0.69 1.23/0.81	1.31−4.7 0.42−1.8 0.9 0.7 0.2	Jorge da Silva (1996); Mazé et al. (1997); Mauritzen et al. (2001); Coelho et al. (2002)
Biscay	8	−4.00E 48.20N	−8.10E 43.10N	$S < 35$ $35 < S < 35.6$ $35.6 < S$	−0.24/0.31 0.04/0.31 0.23/0.55	−0.1−0.1 −0.2−0.0 −2.6−−2.0	Frail-Nuez et al. (2008)
Celtic shelf	9	−10.10E 47.60N	−9.40E 48.40N	$200 < z < 1500$ $200 < z < 3000$	4.31/2.85 4.71/3.49	1 3	Pingree and Le Cann (1990)
Ellett line	10	−7.70E 56.80N	−13.80E 57.50N	$z < 500$ $z < 1200$ $1200 < z < 1800$	2.86/0.54 3.89/0.93 −0.19/0.09	2.5−2.7 3.5−3.7 0.2	Ellett and Martin (1973); Holliday et al. (2000)
St Georges Channel	11	−6.45E 52.30N	−5.10E 51.80N	NO	0.08/0.06	0.18	Brown et al. (2003)
North Irish Sea Channel	12	−5.00E 54.90N	−5.60E 54.60N	NO	0.01/0.05	−0.175−0.14	Howarth (1982); Brown and Gmitrowitz (1995)
Dover Strait	13	1.80E 50.90N	1.35E 51.20N	NO	0.07/0.06	0.094−0.17	Otto et al. (1990); Prandle et al. (1996)

[Title Page](#)
[Abstract](#)
[Introduction](#)
[Conclusions](#)
[References](#)
[Tables](#)
[Figures](#)
[Back](#)
[Close](#)
[Full Screen / Esc](#)
[Printer-friendly Version](#)
[Interactive Discussion](#)


Assessment of the Iberia-Biscay-Ireland configuration

C. Maraldi et al.

Title Page

Abstract

Introduction

Conclusions

References

Tables

Figures

◀

▶

◀

▶

Back

Close

Full Screen / Esc

Printer-friendly Version

Interactive Discussion



Table 4. List of in situ buoys used in this study. For each buoy, the longitude, latitude, and variables available at the station and the organisation providing the data are indicated. The variables that may be available are: sea surface temperature (SST), sea surface salinity (SSS), currents (UV) at the surface for Puertos del Estado buoys, temperature, salinity and currents profiles in the upper 200 m for AZTI buoys and atmospheric variables (AV) that include air temperature, atmospheric pressure and wind velocity. AZTI data include 18-depth levels of measurements in the upper 150 m for the currents (12, 20, 28, 36, 44, 52, 60, 68, 76, 84, 92, 100, 108, 116, 124, 132, 140 and 148 m) and measurements at 10, 20, 30, 50, 75, 100 and 200 m for temperature and salinity.

Mooring name	Lon	Lat	SST	SSS	UV	AV	Organism
Cadiz_Buoy	-6.96	36.48	✓	✓	✓	✓	Puertos del Estado
Cabo Silleiro	-9.40	42.12	✓	✓	✓	✓	Puertos del Estado
Villano Sisargas	-9.21	43.49	✓	✓	✓	✓	Puertos del Estado
Estaca Bares	-7.62	44.06	✓	✓	✓	✓	Puertos del Estado
Cabo Penas	-6.17	43.73	✓	✓	✓	✓	Puertos del Estado
Sanatander	-3.77	43.84	✓	✓	✓	✓	Puertos del Estado
Bilao	-3.04	43.63	✓	✓	✓	✓	Puertos del Estado
Tenerife	-16.58	28.00	✓	✓	✓	✓	Puertos del Estado
Gran Canaria	-15.81	28.19	✓	✓	✓	✓	Puertos del Estado
M1	-11.20	53.13	✓				Marine institute
M2	-5.42	53.48	✓				Marine institute
M3	-10.55	51.22	✓				Marine institute
M4	-10.00	55.00	✓				Marine institute
M5	-6.70	51.69	✓				Marine institute
M6	-15.93	53.06	✓				Marine institute
Brittany	-8.50	47.50	✓				Météo France
Gascogne	-5.00	45.20	✓				Météo France
Lion	4.70	42.10	✓				Météo France
Ouessant	-5.75	48.50	✓				Météo France
Donostia	-2.02	43.56	✓	✓	✓		AZTI
Matxitxako	-2.69	43.63	✓	✓	✓		AZTI

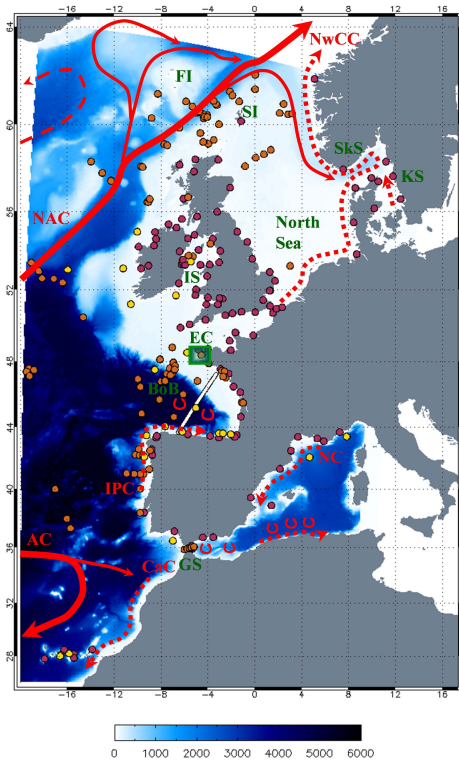


Fig. 1. Bathymetry of the domain [m]. Superposed are the tide gauge positions (red dots), the buoy locations (yellow dots), the current meter data for tidal comparisons (orange dots), the altimeter track crossing the Bay of Biscay (white line) and HF radar surface current measurements off West Brittany (green box). The main surface dynamical features are also shown: the Azores Current (AC), the Canary Current (CaC), The Northern Current (NC), the Iberian Poleward Current (IPC), the Norwegian Coastal Current (NwCC), the North Atlantic Current (NAC). Red symbols represent mesoscale activity in the Mediterranean Sea and in the Bay of Biscay. Some geographical features of the area are also mentioned: the Gibraltar Strait (GS), the Bay of Biscay (BoB), the English Channel (EC), the Irish Sea (IS), the Shetland Islands (SI) and the Faeroe Islands (FI), the Skagerrak Strait (SkS) and the Kattegat Strait (KS).

Assessment of the Iberia-Biscay-Ireland configuration

C. Maraldi et al.

Title Page

Abstract Introduction

Conclusions References

Tables Figures

◀ ▶

◀ ▶

Back Close

Full Screen / Esc

Printer-friendly Version

Interactive Discussion



Assessment of the Iberia-Biscay-Ireland configuration

C. Maraldi et al.

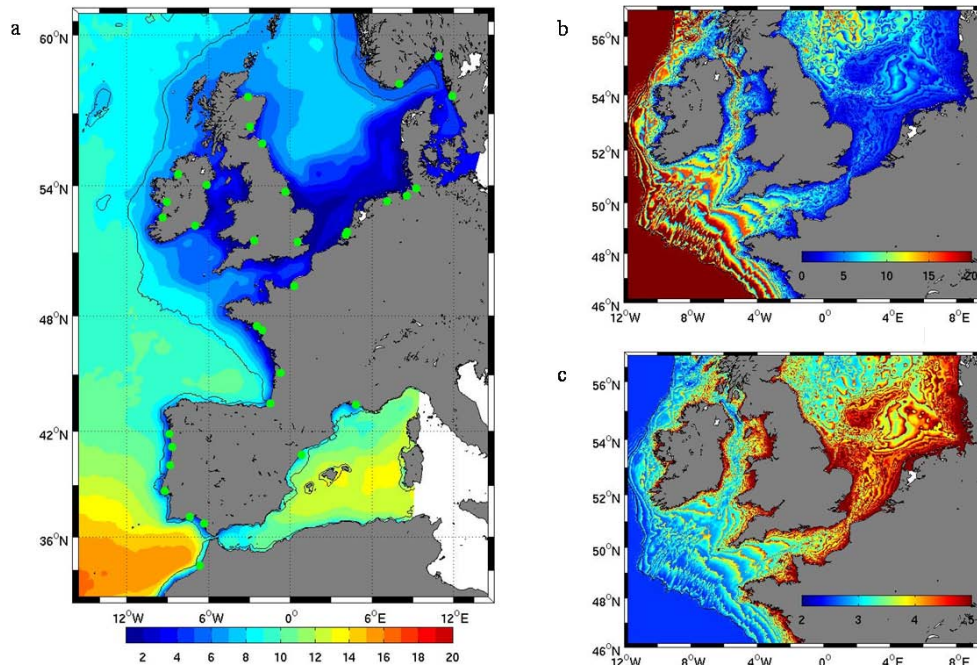


Fig. 2. (a) Annual climatological PAR (Photosynthetically Attenuation Radiation) attenuation depth derived from satellite observations [m]. Green dots correspond to river inputs locations. (b) Partial bottom cell thickness on continental shelves [m]. (c) Bottom drag coefficient C_d according to Eq. (5). On each figure, black thin line is the 200 m isobath.

[Title Page](#)[Abstract](#)[Introduction](#)[Conclusions](#)[References](#)[Tables](#)[Figures](#)[◀](#)[▶](#)[◀](#)[▶](#)[Back](#)[Close](#)[Full Screen / Esc](#)[Printer-friendly Version](#)[Interactive Discussion](#)

Assessment of the Iberia-Biscay-Ireland configuration

C. Maraldi et al.

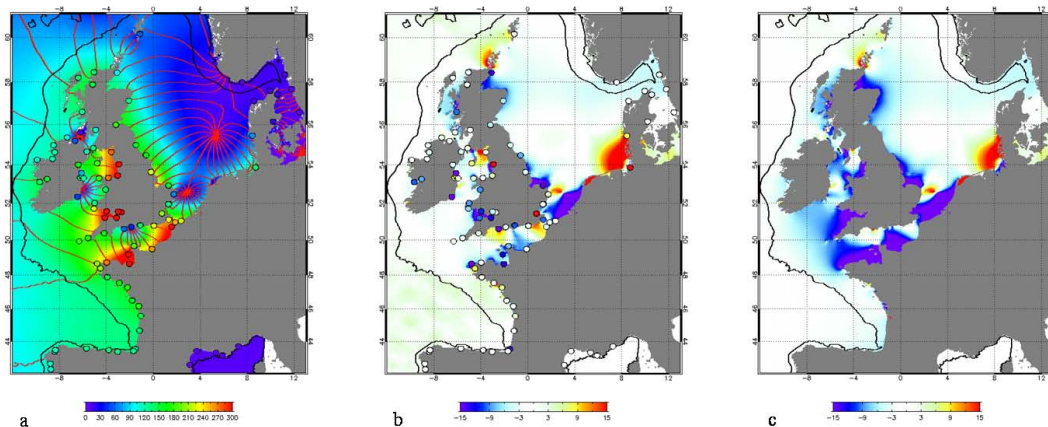


Fig. 3. (a) Amplitude in cm (color) and phase (red lines) of modeled M2 tidal constituent. Overplotted filled dots are the M2 observed harmonic constants at the various tide gauges used for quantitative assessment. (b) M2 Amplitude difference [cm] between the FES2004 solution (Lyard et al., 2006) and the model. Overplotted filled dots represent amplitude and phase differences between tide gauges and the model. (c) Same as (b) but in runbt experiment.

Title Page

Abstract

Introduction

Conclusions

References

Tables

Figures

◀

▶

◀

▶

Back

Close

Full Screen / Esc

Printer-friendly Version

Interactive Discussion



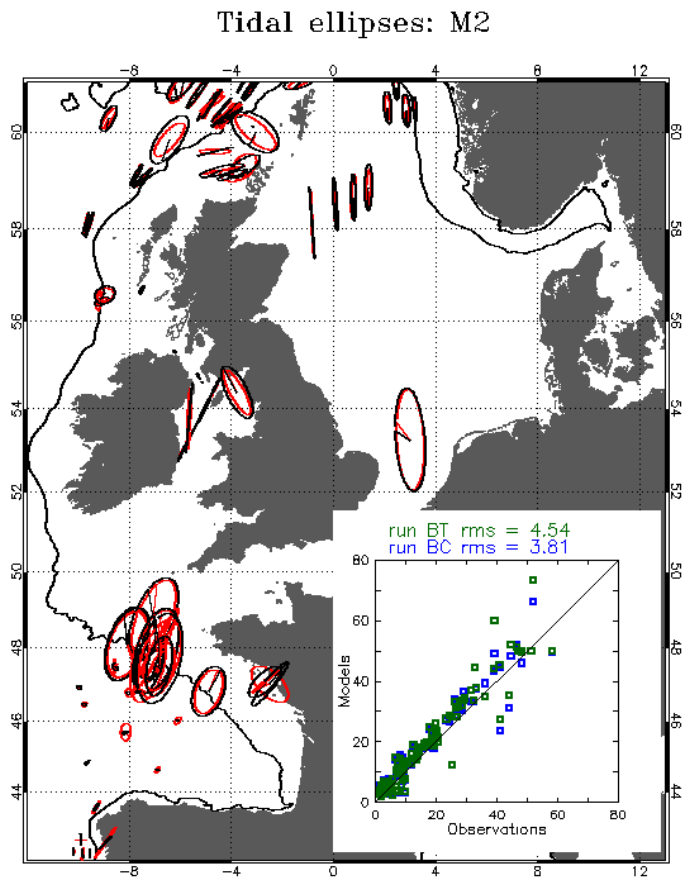
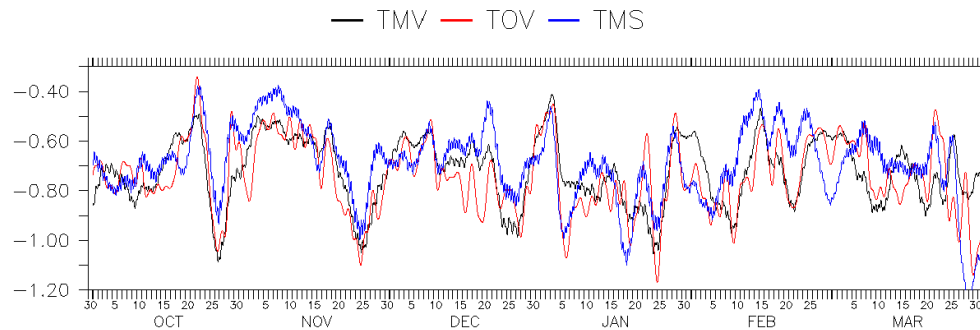


Fig. 4. Comparison of barotropic M2 tidal ellipses to in situ measurements (black for model, red for observations).

Assessment of the Iberia-Biscay-Ireland configuration

C. Maraldi et al.

**Fig. 5.** Transports (outflow) at Gibraltar Strait for TOV, TMV and TMS.

Title Page

Abstract

Introduction

Conclusions

References

Tables

Figures

◀

▶

◀

▶

Back

Close

Full Screen / Esc

Printer-friendly Version

Interactive Discussion



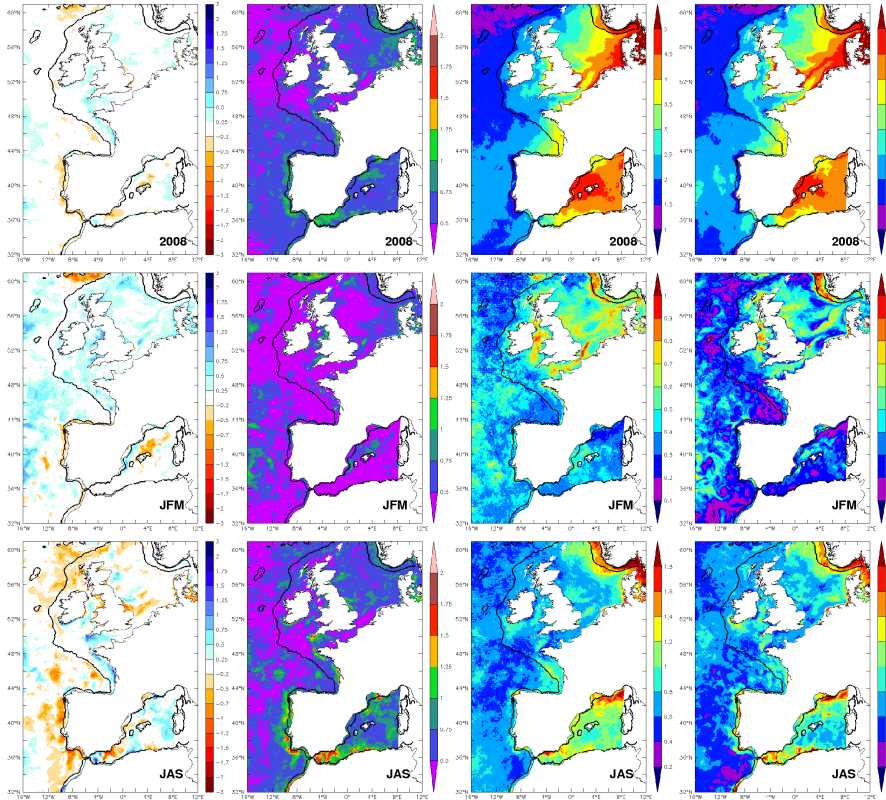


Fig. 6. Comparison to satellite SST observations: From left to right: Bias (model-observation), RMS error, observation standard deviations, model standard deviation. First row shows annual statistics, second winter and bottom row summer.

Assessment of the Iberia-Biscay-Ireland configuration

C. Maraldi et al.

Title Page

Abstract Introduction

Conclusions References

Tables Figures

⏪ ⏩

◀ ▶

Back Close

Full Screen / Esc

Printer-friendly Version

Interactive Discussion



Assessment of the Iberia-Biscay-Ireland configuration

C. Maraldi et al.

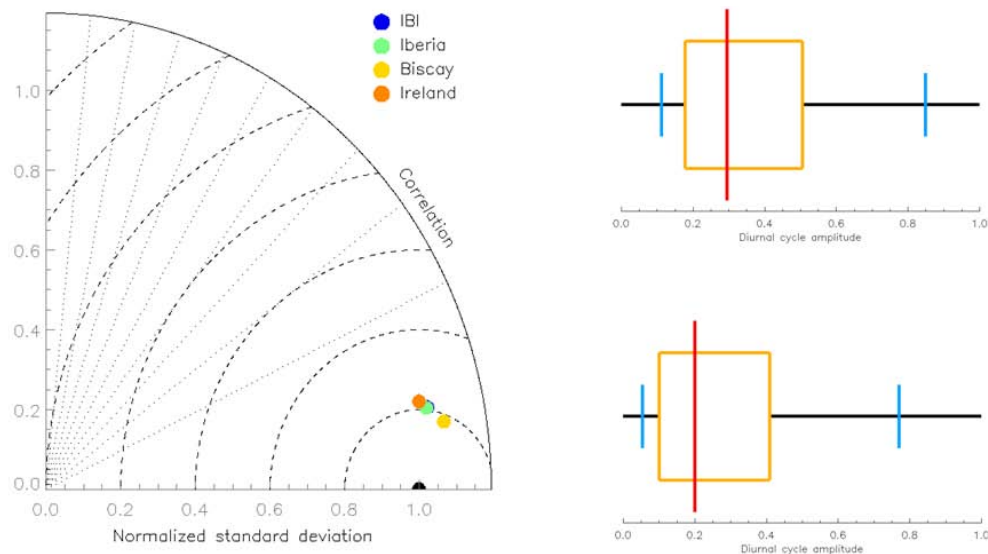


Fig. 7. Left: Taylor diagram of the 1-day low pass filtered SST at buoy locations in different regions. Filled dots are for comparisons with IBI and crosses are for comparisons with PSY2V3. Right: Boxplot of the diurnal cycle computed from data (top) and from model (bottom). The distribution is described with percentiles of data (vertical lines). From the left to the right we indicate the position of the 10th percentile (blue), the lower quartile (yellow), the median (red), the upper quartile (yellow) and the 90th percentile (blue).

Title Page

Abstract

Introduction

Conclusions

References

Tables

Figures

◀

▶

◀

▶

Back

Close

Full Screen / Esc

Printer-friendly Version

Interactive Discussion



Assessment of the Iberia-Biscay-Ireland configuration

C. Maraldi et al.

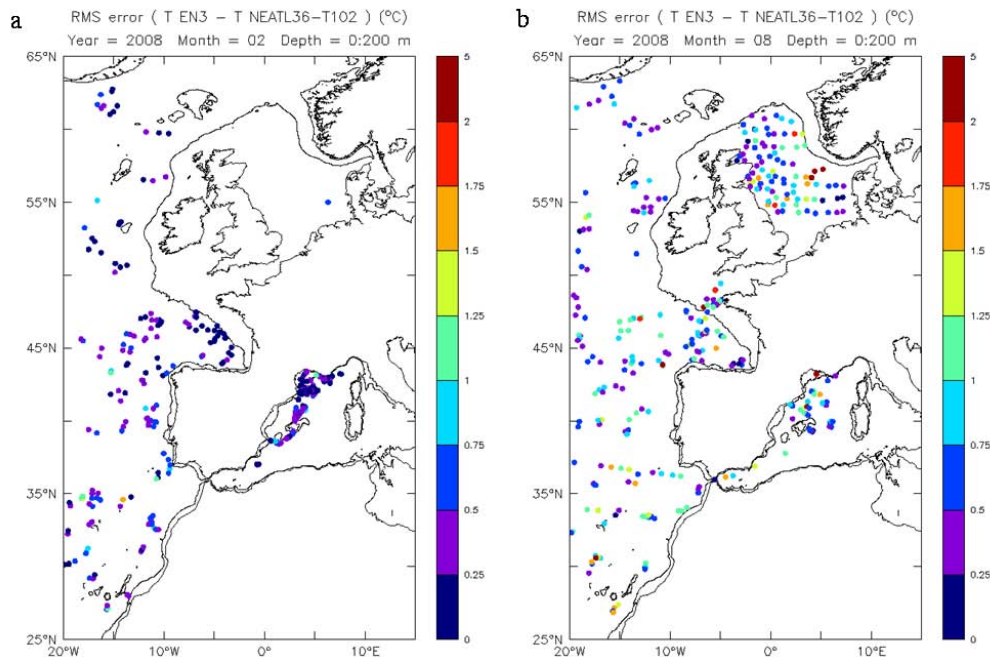


Fig. 8. RMS of temperature differences between EN3 profiles and model profiles computed over the first 200 m. Results are presented for February 2008 (**a**) and August 2008 (**b**).

Title Page

Abstract

Introduction

Conclusions

References

Tables

Figures

◀

▶

◀

▶

Back

Close

Full Screen / Esc

Printer-friendly Version

Interactive Discussion

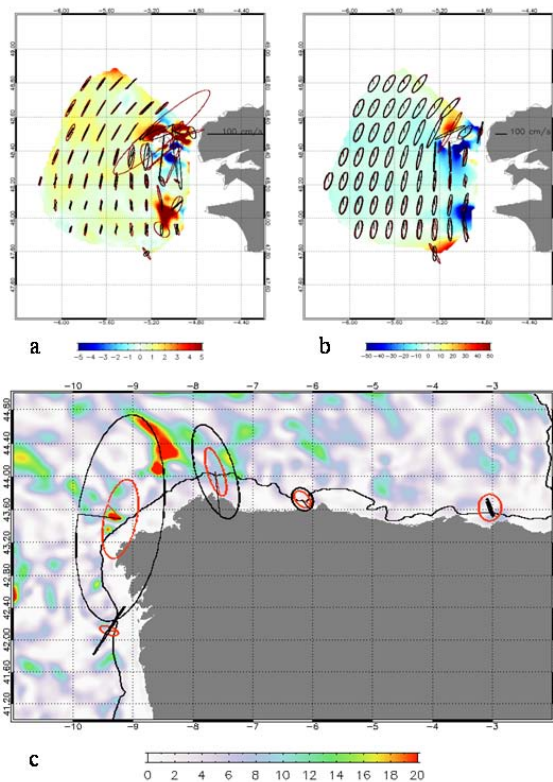


Fig. 9. (a) And (b): M2 **(a)** and M4 **(b)** modeled (black) and observed (red) surface tidal ellipses at HF radar measurements locations. Shaded contours represent the difference Model-observation semi-major axis [cm s^{-1}]. **(c)** Modeled (black) and observed (red) near surface M2 tidal ellipses at Puertos del Estado current meters locations. Shaded contours: M2 surface velocity difference between the run with stratification (runbc) and the run without stratification (runbt).

Title Page	
Abstract	Introduction
Conclusions	References
Tables	Figures
◀	▶
◀	▶
Back	Close
Full Screen / Esc	
Printer-friendly Version	
Interactive Discussion	



**Assessment of the
Iberia-Biscay-Ireland
configuration**

C. Maraldi et al.

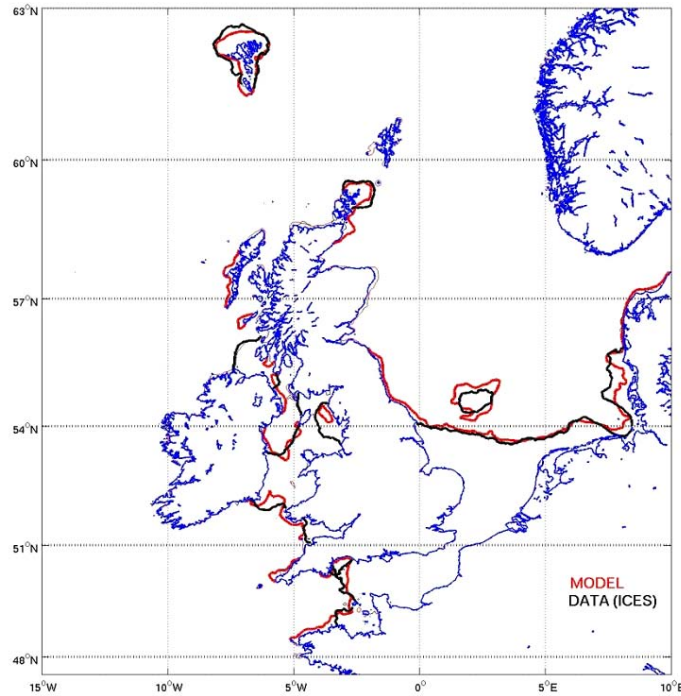


Fig. 10. Summer (June, July, August) tidal fronts positions as deduced from surface to bottom temperature difference ($T = 0.5^\circ\text{C}$) from the model (red) and from ICES data (black).

Title Page

Abstract

Introduction

Conclusions

References

Tables

Figures

◀

▶

◀

▶

Back

Close

Full Screen / Esc

Printer-friendly Version

Interactive Discussion



**Assessment of the
Iberia-Biscay-Ireland
configuration**

C. Maraldi et al.

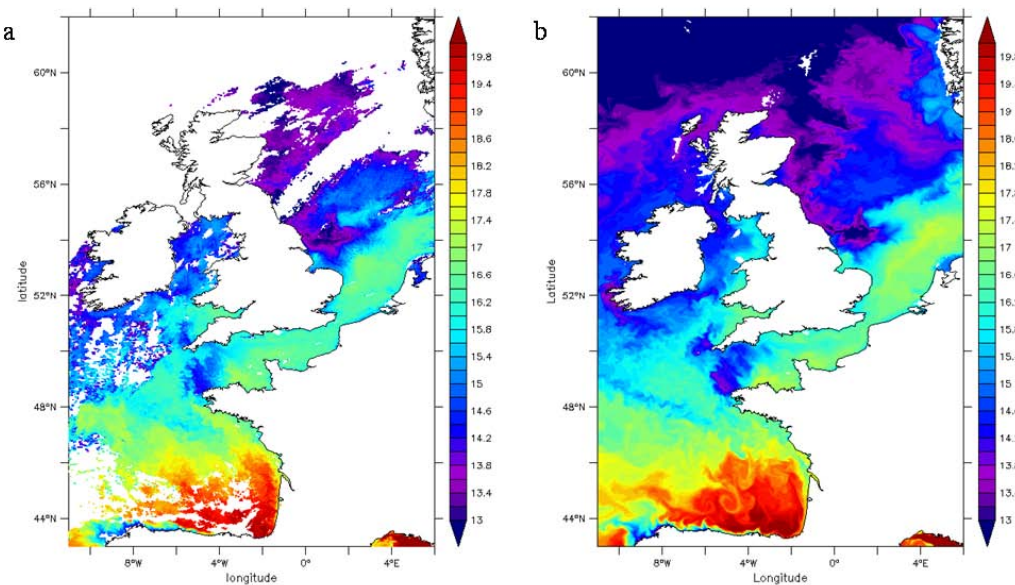


Fig. 11. Sea surface temperature (°C) from MODIS data **(a)** and from the model **(b)** on 27 September 2008.

Title Page

Abstract

Introduction

Conclusions

References

Tables

Figures

◀

▶

◀

▶

Back

Close

Full Screen / Esc

Printer-friendly Version

Interactive Discussion



Assessment of the Iberia-Biscay-Ireland configuration

C. Maraldi et al.

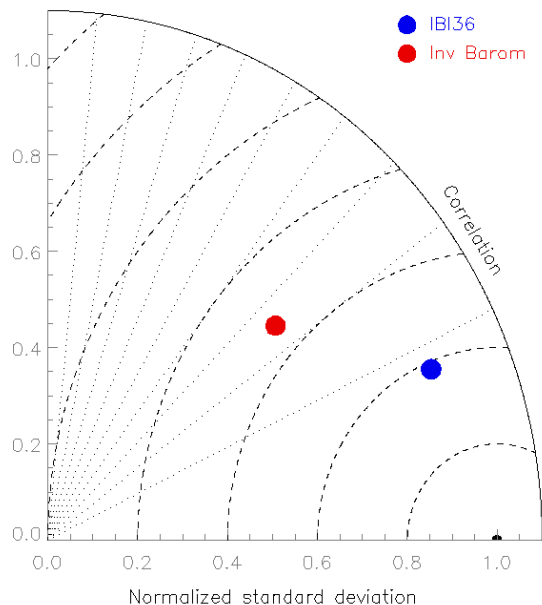


Fig. 12. Taylor diagram for comparisons between tide gauge data and the model residual elevations (blue) and the inverse barometer (red). Results are computed for periods below 10 days and for data located in the Bay of Biscay and in the English Channel. The radial coordinate indicates the standard deviation normalized by the data standard deviation; the concentric circles represent the RMS differences for time series normalized by the data standard deviation (the observations are indicated with the black point) and the angular coordinate represents the correlation with observations.

Title Page

Abstract

Introduction

Conclusions

References

Tables

Figures

⏪

⏩

◀

▶

Back

Close

Full Screen / Esc

Printer-friendly Version

Interactive Discussion



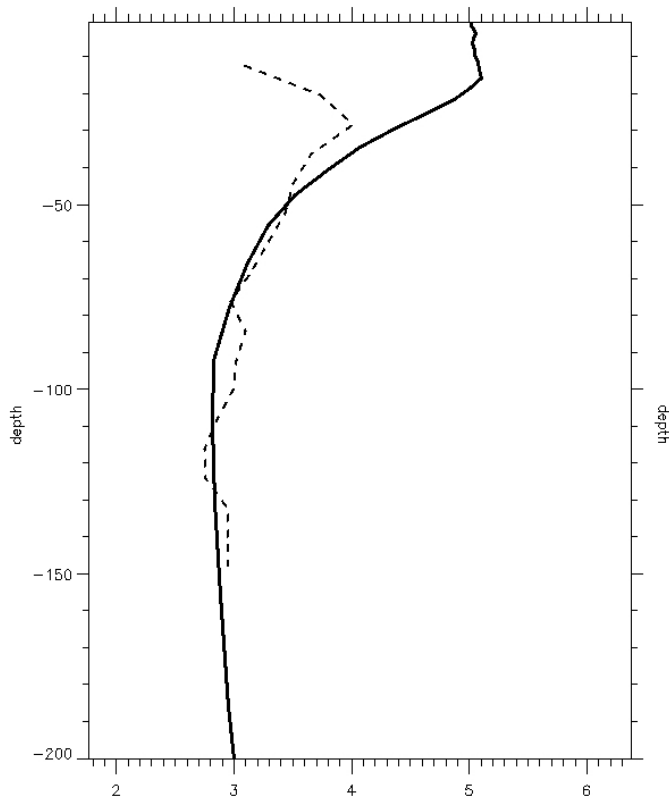


Fig. 13. Vertical profiles of the M2 semi major axis as observed (dashed line) and modelled (full line) at the Matxitxako buoy location.

Assessment of the Iberia-Biscay-Ireland configuration

C. Maraldi et al.

Title Page	
Abstract	Introduction
Conclusions	References
Tables	Figures
⏪	⏩
◀	▶
Back	Close
Full Screen / Esc	
Printer-friendly Version	
Interactive Discussion	



Assessment of the Iberia-Biscay-Ireland configuration

C. Maraldi et al.

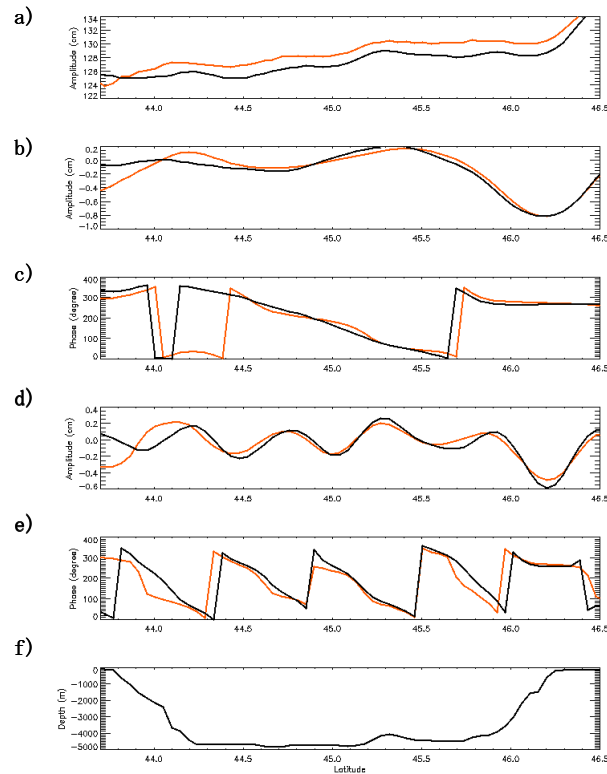


Fig. 14. (a) Along track amplitudes (cm) deduced from the M2 harmonic analysis of altimetric data (red) and model (black). (b) Baroclinic amplitudes in cm and (c) phase of the residual tides for the altimetric data (red) and the model (black) and for the first baroclinic mode. (d) Baroclinic phased locked elevations in cm and (e) phase of the residual tides for the altimetric data (red) and the model (black) and for the second baroclinic mode. (f) Along track bathymetry (m).

Title Page

Abstract

Introduction

Conclusions

References

Tables

Figures

◀

▶

◀

▶

Back

Close

Full Screen / Esc

Printer-friendly Version

Interactive Discussion



Assessment of the Iberia-Biscay-Ireland configuration

C. Maraldi et al.

Title Page

Abstract

Introduction

Conclusions

References

Tables

Figures

◀

▶

◀

▶

Back

Close

Full Screen / Esc

Printer-friendly Version

Interactive Discussion

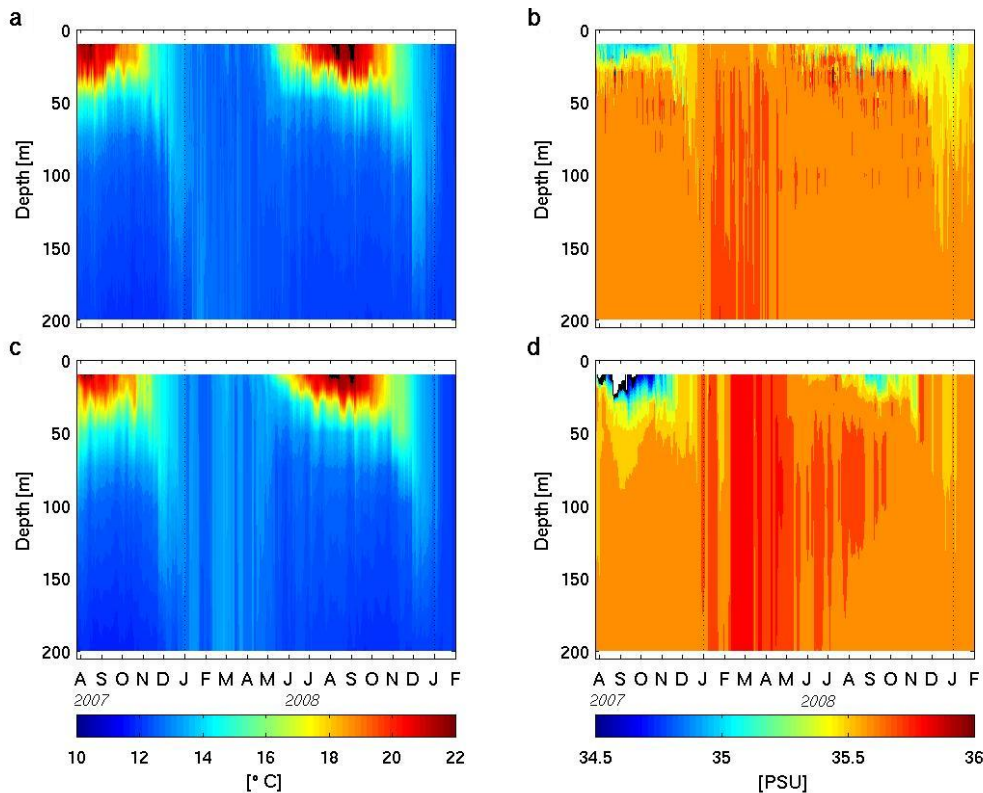


Fig. 15. Temperature and salinity profiles in the upper 200 m at station Matxitxako as a function of time (August 2007 to February 2009) from the observations (**a**, **b**) and from the model (**c**, **d**). As no measurement is available above 10 m, we show the model results below 10 m.

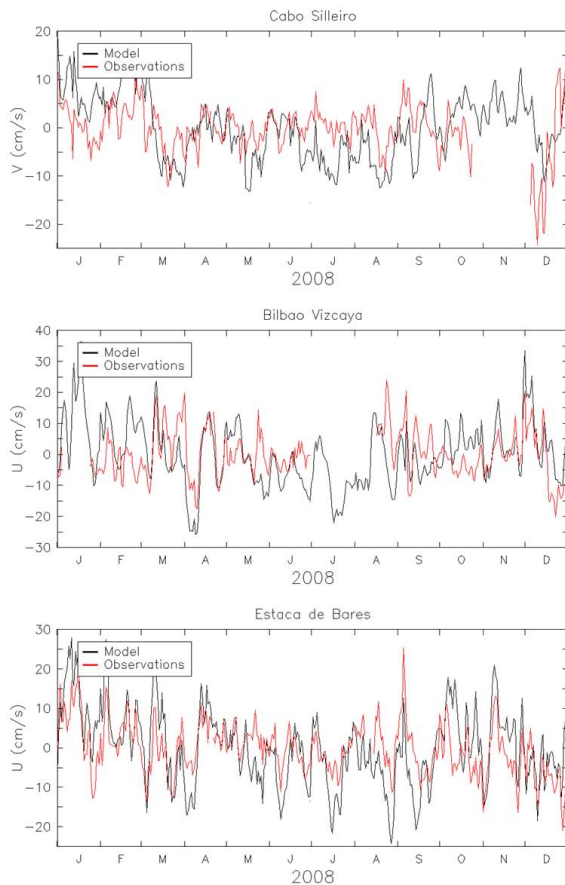


Fig. 16. Modelled (black) and observed (red) residual near surface velocity (approximately along slope) at various moorings along the Iberian slope: northern component at Cabo Silleiro and eastward component at Escata de Bares and Bilbao.

**Assessment of the
Iberia-Biscay-Ireland
configuration**

C. Maraldi et al.

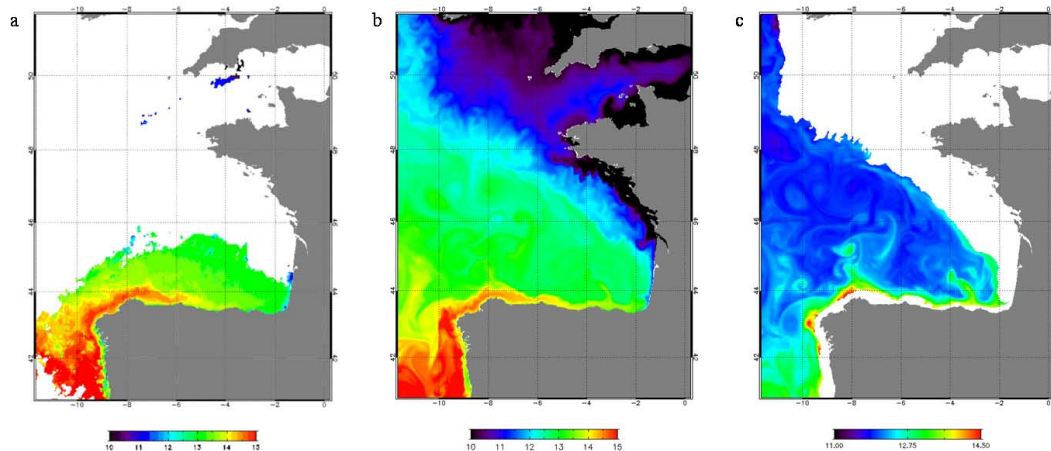


Fig. 17. Sea surface temperature ($^{\circ}\text{C}$) from AVHRR data **(a)** and from the model **(b)** the 20th of January 2008. Modelled temperature at 200 m the 20th of January 2008 **(c)**.

Title Page

Abstract

Introduction

Conclusions

References

Tables

Figures

◀

▶

◀

▶

Back

Close

Full Screen / Esc

Printer-friendly Version

Interactive Discussion



Assessment of the Iberia-Biscay-Ireland configuration

C. Maraldi et al.

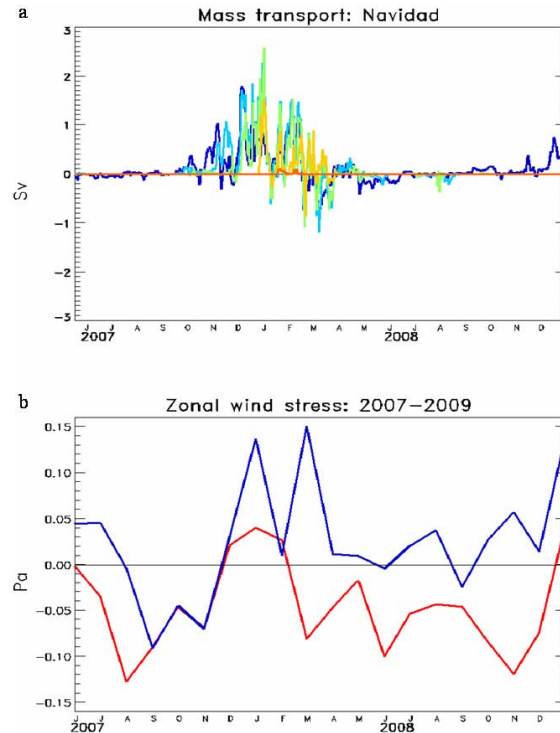


Fig. 18. (a) Transport of the poleward flow for water mass warmer than 13.0°C and saltier than 35.7 psu at 43.24° N (blue), at 7.61° W (turquoise blue), at 6.2° W (green), at 3.8° W (yellow) and at 44.4° N (orange). (b) Meridional wind stress τ_y off western Iberia (red) and of the zonal wind stress τ_x off northern Iberia (blue). Boxes chosen for the spatial average of τ_x and τ_y have been chosen following the study of Le Cann and Serpette (2009).